BIOADHESIVES FOR SOFT TISSUE INTEGRATION

M.Sc. Thesis

By
Vinod Yadav

DEPARTMENT OF BIOSCIENCES AND BIOMEDICAL ENGINEERING
INDIAN INSTITUTE OF TECHNOLOGY INDORE
JUNE, 2023

BIOADHESIVES FOR SOFT TISSUE INTEGRATION

A THESIS

Submitted in partial fulfillment of the requirements for the award of the degree
of
Master of Science

by
VINOD YADAV

DEPARTMENT OF BIOSCIENCES AND BIOMEDICAL ENGINEERING

INDIAN INSTITUTE OF TECHNOLOGY INDORE

JUNE, 2023

INDIAN INSTITUTE OF TECHNOLOGY INDORE

CANDIDATE'S DECLARATION

I hereby certify that the work which is being presented in the thesis entitled **BIOADHESIVES FOR SOFT TISSUE INTEGRATION** in the partial fulfillment of the requirements for the award of the degree of **MASTER OF SCIENCE** and submitted in the **DEPARTMENT OF BIOSCIENCES AND BIOMEDICAL ENGINEERING, Indian Institute of Technology Indore**, is an authentic record of my own work carried out during the time period from June 2021 to June 2023 under the supervision of Dr. Sunil Kumar Boda, Assistant professor, BSBE, IIT Indore.

The matter presented in this thesis has not been submitted by me for the award of any other degree of this or any other institute.

Vinod yadav

Signature of the student with date
(Vinod Yadav)

This is to certify that the above statement made by the candidate is correct to the best of my/our knowledge.

Signature of the Supervisor

(Dr. Sunil Kumar Boda)

Vinod yadav has successfully given his/her M.Sc. Oral Examination held on **9 May, 2023**.

Signature(s) of Supervisor(s) of MSc thesis
(Dr. Sunil Kumar Boda)
Date:

P.V. Kodgire

Convener, DPGC
(Prof. Prashant Kodgire)
Date:

Signature of PSPC Member
Prof. Avinash Sonawane
Date:

Parimalkar

Signature of PSPC Member
Dr. Parimal Kar
Date: 10/5/2023

---

v

ACKNOWLEDGEMENTS

The unmatched beauty of science lies in fact that it is never static, never firm but has immense flexibility to experiment about it. It does not need to be true completely or partially. It is the desire of human race to define the phenomenon surrounding them with best of their current knowledge and the resources available at time and with improvement in these, this understanding further deepens sometimes supporting the previously known facts and other times contradicting the same, both of which are equally important.

I would like to express my sincere gratitude for this moment of accomplishment to my supervisor Dr Sunil Kumar Boda for accepting me in his lab for my M.Sc. thesis project work. This one year was full of hard work, stress, happiness, failures. But his continuous guidance timely advice, scientific approach, and support always helped in moving forward. I am indebted to him for always finding time between their busy schedules to discuss my results and clear my doubts. Without their guidance and persistent help, this project would not have been possible within the limited time frame.

I would also like to thank my PSPC members Prof. Avinash Sonawane and Dr. Parimal Kar for their critical comments pointing out the areas I can improve upon how to make better scientific figures, how to write a better thesis, how give a good presentation. Even after having different research field, they took time and read my unsatisfactory and incomplete work and sill gave so much of important comments that are the reason my thesis could be completed in time.

I would humbly like to express my gratitude to H.O.D and all the faculty members of BSBE who were so much sympathetic towards all students and we all had freedom to approach any of the teacher for discussing our problems and it has helped me a lot. Specially Dr. Sharad Gupta for letting me use instruments in his lab, Prof. Prashant Kodgire who gave his very helpful suggestions about how can I improve my SDS PAGE results also Dr. Parimal Kar for allowing me to access his lab for my computational work

I would like to express my deep gratitude to my lab seniors Sangeeta Shrivas and Pallavi Seal, for all the scientific discussion and for keeping me motivated, energetic and always there for their kind support and valuable time. They have taught me very simple techniques also arranged the different slots even when they were also having so much burdened.

Nevertheless, I would like to thank all my batchmates for keeping me motivated, energetic and enthusiastic for every upcoming hurdle, my friends Rahul, Abhijeet, Tanisq, Junaid, Yogesh, Nikhil, Siddharth, Vaibhav who are like my family away from home.

I would like to express my deep gratitude to the source of my life, my parents. My father, Mr. Suresh Yadav, and my mother, Mrs. Shobha Devi for their unconditional love, care, support and without them, I would not be here where I am today. Finally, I would like to thanks Almighty God for granting me strength and health and all others who knowingly or unknowingly helped me in this journey.

VINOD YADAV

DEDICATED

TO

ALMIGHTY

GOD

Abstract

This thesis work revolves around preparing a hydrogel-based biomaterial that can facilitate the skin cells sealing around percutaneous osseointegrated prosthesis. Osseointgerated prosthesis mostly made of the titanium metal due to its inertness and biocompatibility suffers from limitation of integrating with the skin cells due to foreign body reaction and lesser hemidesmosomal junction formation between the cells and the implant, commonly called epithelial down growth. Due to this a gap is left between the implant and skin leading to the loosening of the implant and paving the way to pathogen attack which further worsen the situation and ultimately the implant needs a revision surgery or replacement. To seal this gap the traditional suturing and stapling methods are also not effective due to its location. A new approach of using some type of hydrogel-based adhesive can be good alternative. Hydrogel based bandages and scaffolds have already been in use for injury repair and sealing of wounds. The hydrogels commonly in use are synthetic polymer based like the cyanoacrylate though these possess very good mechanical properties still this produce toxic compound upon their degradation, so using some bio-polymer like protein or a carbohydrate is a practical solution. However, the naturally crosslinked polymers are not that good biomaterials. Some crosslinker like the catechol group containing polyphenols (Dopamine and Quercetin) have been tried human hair keratin was chosen. Due to its cheap availability form different waste sources and good biocompatibility Keratin also belong to the epithelial. Keratin was extracted and characterized then a hydrogel was prepared using a combination of both physical (freeze thaw) and chemical crosslinking mechanism (Michael addition using polyphenols i.e., quercetin and dopamine). Hydrogel was then analyzed and tested for its structure swelling capabilities and cytocompatibility and for its ability to hold the cells.

TABLE OF CONTENTS

LIST OF FIGURES

LIST OF TABLES

LIST OF ABBREVIATIONS

ITAP Intraosseous Transcutaneous Amputation Prosthesis

HK Human Hair Keratin

Ti Titanium

PEG Polyethylene Glycol

PAA Polyacrylamide

GA Glutaraldehyde

2D Two Dimensional

3D Three Dimensional

CD Circular Dichroism

SEM Scanning Electron Microscope

IR Infrared Radiation

mQ Mili Q

SDS PAGE Sodium Dodecyl Sulphate - Polyacrylamide Gel Electrophoresis

DNTB 5,5′-Dithiobis (2-Nitrobenzoic Acid)

DMEM Dulbecco's Modified Eagle's Medium

kDa Kilo Dalton

Chapter 1

Introduction

1.1 Percutaneous Devices

Percutaneous artificial medical devices are the structure made of some biocompatible material like metal and alloys, these are placed inside the body through a surgically created integumental (skin) defect. These provide a direct connection of the body's internal structure to outside and thus are helpful in diagnosis, monitoring, treatment [1]. These constitute a broad class of structures like needle type glucose sensors which provide a real time monitoring of the blood glucose concentration, through a subcutaneous needle placed Transdermally and it can give in real time the glucose concentration. Structure as the catheters are used for draining fluids form the body most common of these is the urinary catheres help patients with urethral blockage or injury to pass urine for the blader with help of a tube directly inserted into urethra, surgical operations that need to access small blood vessel like cardiac surgeries also use surgical catheters [2]. Osseointegrated prosthetic limbs and dental implants represent a very special class of percutaneous devices and are permanent placed through skin. As all these structures remain in prolonged contact with body these need to be very compatible to the body, thus these are fabricated with some biodegradable and compatible materials like silicones, metals, and their alloys.

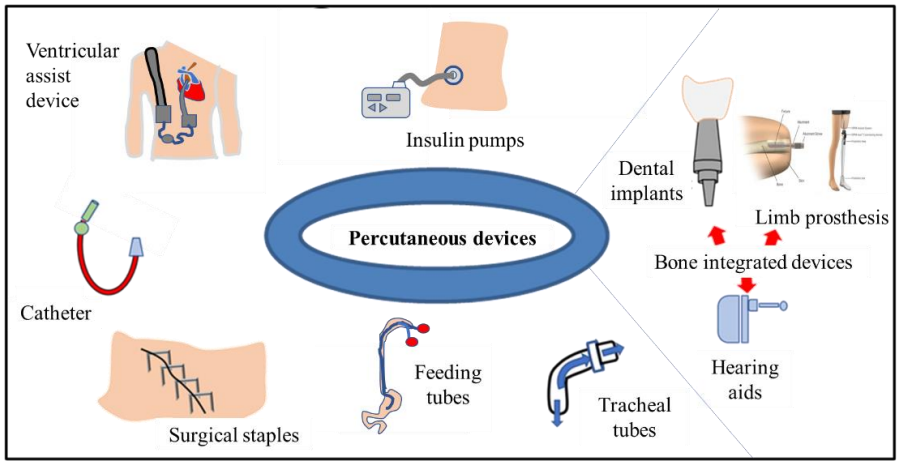

Figure 1.1: Different types of percutaneous devices [3].

1.2 Osseointegrated prosthesis

It is yet another class of the percutaneous device permanently disrupting the skin barrier. Here the implant generally made of some metal or alloy like Ti (due to its inertness and biocompatibility) is directly fixed into the bone [4], while its abutment is protruding through the skin to external fixtures that can attach to a prosthetic limb (**Figure: 1.2**.) The concept of osseointegration was first introduced by Per-Ingvar Branemark (1969) and defined by him as "**A direct structural and functional connection between ordered living bone and the surface of the load**" [5]. He also was the first to demonstrate successful osseointegrated dental implants. Since then, several implant and prosthesis to promote osseointegration have been developed. Most common are the intraosseous transcutaneous amputation prosthesis (ITAP), these have come up as an alternative to the socket-based prosthesis for the limb amputees (where a limb or its part is removed due to injury, trauma, war, etc.) and offers numerous advantages over the later as enhanced osseo-perception, improved limb movements, better mechanical load transfer, etc [6].

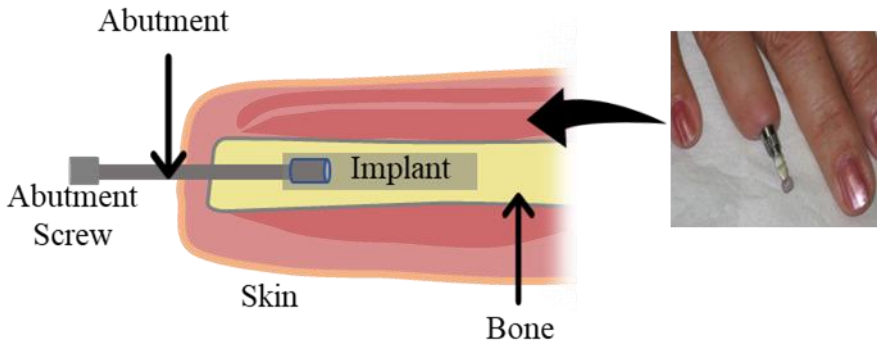

Figure 1.2: Components of an osseointegrated prosthesis – implant abutment and abutment screw [7].

1.3 Epithelial marsupialization around percutaneous implants

It is the downgrowth of the epithelial cells along the surface of the implant without actual physiological connection to it, due to its foreign nature and non-remodelling structure. It leads to the creation of the

moist gaps at the interface between the skin and implant, thus serving as a site for the bacterial/fungal proliferation. This causes infection and implant loosening and ultimately failure of these permanent percutaneous devices necessitating replacement or removal [8]. Such revision surgeries cause less successful and add additional burden on patient economically. As an example, around one million dental implants fail worldwide, also catheters, which are left in place permanently in some cases, demonstrate 80,000 infections per year [9].

1.4 Natural Percutaneous Structures

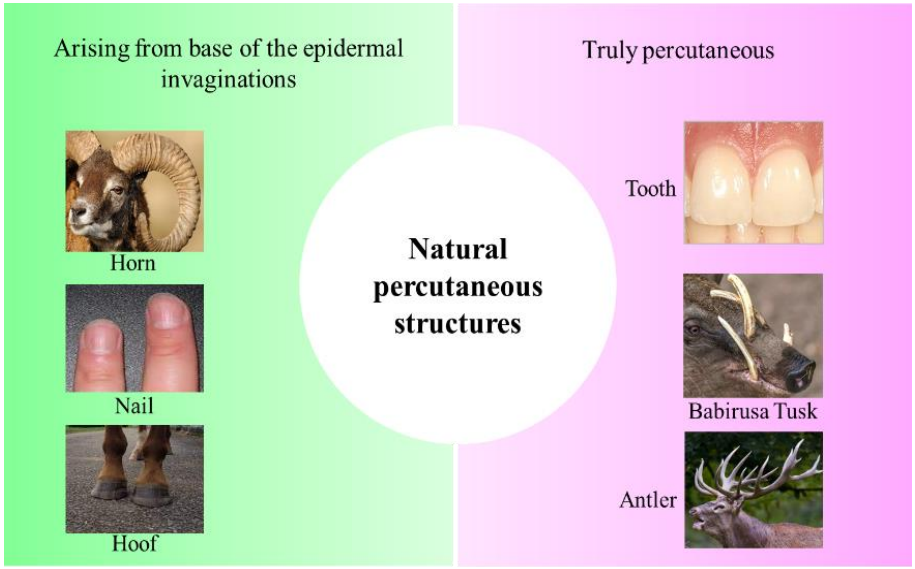

Figure 1.3: Percutaneous structures in nature[10].

Animal and human body have a number of structures which arising from body's internal to outside either by breaking the epithelial barrier also called the true percutaneous like the babirusa tusk, tooth, antlers, etc. as shown in **Figure 1.3.** Other category are the ones that arise from the base of the epidermal invaginations like horns, hoofs, nails, feathers, etc. All these structures however, are tightly sealed with the surrounding skin cells due to presence of a junctional epithelial covering these structures as in tooth that during its development, it secretes a junctional epithelial layer which mediates the formation of the hemidesmosomes that, mediate the cell to the matrix interaction thus binding the

surrounding skin. Most of the modern-day approaches to deal with epithelial downgrowth is to alter the implant surface physiochemical properties and topography, which can lead to enhanced hemidesmosome formation. One way is to coat the implant surface with some biomimicking material [11].

1.5 Problems with currently used methods to seal skin with implants

Commonly used method to seal the skin tissue around the abutment portion of the implant is suturing the skin to the periosteum of the bone (which is the thin layer of soft connective tissue over bone) to create a cuff which prevents the bacterial entry into the site. Sometimes a healing cap or abutment can be placed over the actual abutment part of the implant [12]. However, these methods are slow and healing takes lot of time and the chances of infection in this time frame is very high. Also, the invasive nature of suturing again makes it a less humane and unpreferable option for many, especially patients who are already immune deficient [13].

1.6 Hydrogel based bioadhesives to seal soft tissues around metallic prosthesis

Hydrogel based adhesives are the promising solution to wound healing, and as tissue sealant, due to their ability to stick to biological tissues. These have already been in use as a skin wound sealing, surgical incision closure and internal damage [14]. Hydrogels are the only practical solution while dealing with the fragile tissues or some inaccessible body part where, suturing, or other methods are not effective. A good adhesive could even eliminate the need for sutures completely reducing the scar formation after healing is done. Xinchen Du et. al. prepared one such hydrogel adhesive patch using a combination of chitosan, Poly (ethylene glycol), Diacrylate (PEGDA)

and Tannic Acid crosslinked by UV-light which reported to possess better wet adhesion due to mussel mimicking catechol [15] besides their topical applications. Injectable hydrogel adhesives have shown ability to stop the bleeding due to vessel rupture. Yi Hong et. al reported use of methacrylate gelatin-based hydrogel for sealing the arterial damage, intracavitary haemorrhage or injuries involving essential tissues/organs [16]. Their ability to bind to different synthetic materials such as implantable metals like Ti, Stainless steel, etc. has been found useful to implant fixation in the body. Catechol adhesion mechanism mimicking the mussel foot protein adhesive has inspired many such hydrogels to promote the implant healing. Mihaela Mateescu et. al. prepared an alginate hydrogel modified with catecholate providing a very good adhesion to Ti metal and to pig's gingiva layer [17]. Coating orthopedic implant surface with antimicrobial and osteoconductive has been reported to prevent bacterial biofilm formation and improving the osteogenesis by increasing the mesenchymal cell proliferation [18]

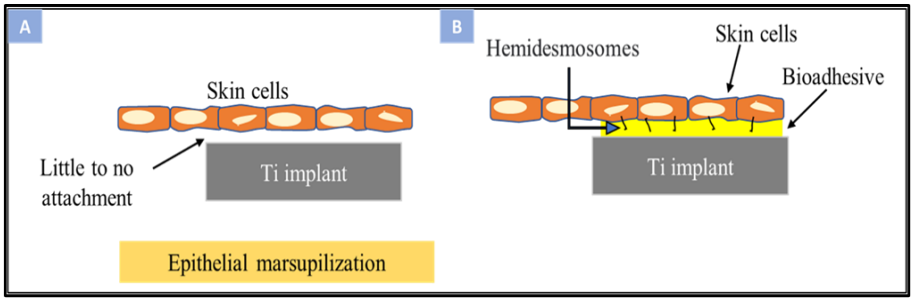

Figure 1.4: Interaction of the titanium prosthesis with the skin cells (A) Epithelial downgrowth (B) Adhesive hydrogel material to hold the cells in place by formation of hemidesmosomes.

1.7 Objectives

- Extraction and characterization of the keratin from human hair
- Formation of hydrogel from the hair keratin and polyphenols (Dopamine and Quercetin)
- Rheological, injectability and tissue adhesive characterization of the hydrogel along with cytocompatibility testing

1.8 Organization of the thesis

This thesis is divided into 5 chapters

1.Chapter1: Introduction of percutaneous implant and their complication

2. Chapter 2: Materials and methods used to carry out this research work

3. Chapter 3: Results and Discussions

4. Chapter 4: Summary

5. Chapter 5: References

Chapter 2

Literature Review

2.1 Introduction to hydrogels

Hydrogels are porous structures which are insoluble in nature. Hydrogel can be formed from synthetic material or from naturally occurring polymer. Due to their excellent porous property and biocompatibility, it makes them the choice of material for medical application. Additionally, it's biodegradability, hydrophilicity, viscoelasticity, softness properties are more suited which can mimic the environment of living tissue [19]. Hydrogels have a more fragile structure, and this depends on the composition and crosslinker used. The more commonly used synthetic polymer to form a hydrogel are polyethylene glycol, polyacrylamide (PAA) which show a great mechanical property like swelling, high strength, and reforming ability. Some of the commercially available synthetic hydrogels are listed in the **table 1**. But major limitations of synthetically derived hydrogel which hinder their use in the medical application are its biocompatibility issue and release of toxic by-product upon degradation in the host system. Accordingly, there have been efforts to develop hydrogel derived from natural polymer such as protein and polysaccharide-based hydrogels [20]. Natural polymer-based hydrogels are nontoxic in nature and mimic the host system which are major characteristics to use in any type of material. Protein like silk, elastin, gelatin, Bovine Serum Albumin (BSA) etc. and polysaccharides such as chitosan and alginate are commonly used hydrogels listed in the literature. To enhance the mechanical strength of naturally derived hydrogel, hybrid hydrogel is formed by combination of both synthetic and natural polymers and generally conjugation or polymerization approaches are used to synthesize the hybrid hydrogel [21].

Table 1: Polymeric hydrogels and their applications.

S. No.	Polymer	Medical application	References
1.	Dextran	Targeted drug delivery to colon tissue	[22]
2.	PHEMA Poly (2-hydroxyethyl methacrylate)	Ocular contact lens synthesis loaded with drug for ocular delivery	[23]
3.	Chitosan	Wound dressing, tissue engineering, drug delivery	[24],[25]
4.	Alginate	emulsions stabilizers, suspenders, tablet binders, delivery of drug in cancer patients	[26]
5.	Alginate-Gelatin hydrogel s	Use as Bio ink for 3D printing scaffolds	[27]
6.	Chitosan/PVA hydrogel	Fabrication of an antimicrobial hydrogel nano fiber mat for wound dressing	[24]
7.	Hyaluronic acid, Glycol chitosan	For in situ repair and stability to the damaged heart tissue post infraction	[28]

2.2 Hydrogel based bioadhesives

Hydrogels are very good bioadhesive candidates due to numerous reactive functional groups on the polymers constituting them [29], which can bind to different tissues by the covalent and non-covalent interactions. Combined with their swelling ability and the hydrated porous nature makes them mimic the biological living tissues with good elasticity, also their porous structure has been used for loading drug [30] and cells [31] for regenerative and antimicrobial therapies. Injectable hydrogels are especially useful as bioadhesive for using in vessel rupture of the cavity damage where normal access is very difficult [32]. Yet another benefit of hydrogels is their tuneable mechanical properties depending upon the polymer crosslinking, chemical composition, crosslinking density, or surface modifications. This allows for customization based on specific tissue types and desired bonding strength.

2.3 Hydrogel based bioadhesives for soft and hard tissue integration

Hydrogels have been recognized as promising materials for tissue engineering and regenerative medicine because of their unique properties, including biocompatibility, biodegradability, and water retention capabilities. The extracellular matrix (ECM) of natural tissues can be mimicked by hydrogels, which can make it easier to integrate the hydrogel with the host tissue, different uses of bioadhesives are given in **figure 2.1**.

(a). Hydrogels for Soft Tissue Integration:

Soft tissue includes skin, cartilage and organs which are composed of complex extracellular matrix that provide the structural organization, biochemical instruction for cell communication and mechanical support. Hydrogel can be synthesized by incorporating various biomolecules such as peptides, peptidoglycan, and growth factor, into

the hydrogel matrix to mimic the ECMs to provide the native environment for the cell adhesion [33]. Some of the hydrogel composed of polyethylene glycol (PEG) and chondroitin sulfate have been developed for cartilage tissue engineering. One of the major structural proteins of ECM is chondroitin sulfate and found to be involved in enhancing the chondrogenesis of encapsulated stem cells [34] Moreover, collagen and hyaluronic based hydrogel have been used for the regeneration of skin due to their native behaviour.

Hydrogels can be functionalized with adhesive peptides such as RGD (Arg-Gly-Asp) and YIGSR (Tyr-Ile-Gly-Ser-Arg) to promote cell adhesion and spreading in addition to ECM mimicking. Adhesive peptides can be incorporated into the hydrogel matrix or immobilized on the hydrogel's surface using a variety of chemical and physical methods [35].

(b). Hydrogels for Hard Tissue Integration:

Hard tissues possess multifaceted structures of hierarchy that provide mechanical support and mineralized matrix for cell attachment and mineralization. By incorporating minerals such as calcium phosphate and hydroxyapatite into the hydrogel matrix, hydrogels can be designed to mimic the micro- and nanostructure of hard tissues [36]

For bone tissue engineering, gelatin and hydroxyapatite hydrogels have been used. The hydroxyapatite replicates the mineralized matrix of bone, while the gelatin serves as a biocompatible and biodegradable matrix for cell adhesion and growth. Similarly, poly (lactic-co-glycolic acid) (PLGA) and calcium phosphate hydrogels have been used for tooth regeneration [37]. Cell proliferation ability of Hydrogels can be enhanced with bioactive molecules such as growth factors and bone morphogenetic proteins (BMPs) to promote osteogenesis and mineralization in addition to mineral mimicking. Various chemical and physical strategies can be used to incorporate these bioactive molecules into the hydrogel matrix or immobilize them on the hydrogel's surface [38].

(c). Hydrogels for Soft and Hard Tissue Integration:

Hydrogels can also be designed to integrate with both soft and hard tissues, such as in the case of cartilage-bone interface regeneration. Hydrogels composed of poly (vinyl alcohol) (PVA) and hydroxyapatite have been developed to promote the integration of cartilage and bone tissues. The PVA mimics the soft tissue matrix of cartilage, while the hydroxyapatite mimics the mineralized matrix of bone [39]. The hydrogel can be loaded with growth factors and chondrocytes to promote cartilage regeneration, while also promoting soft tissue healing around it.

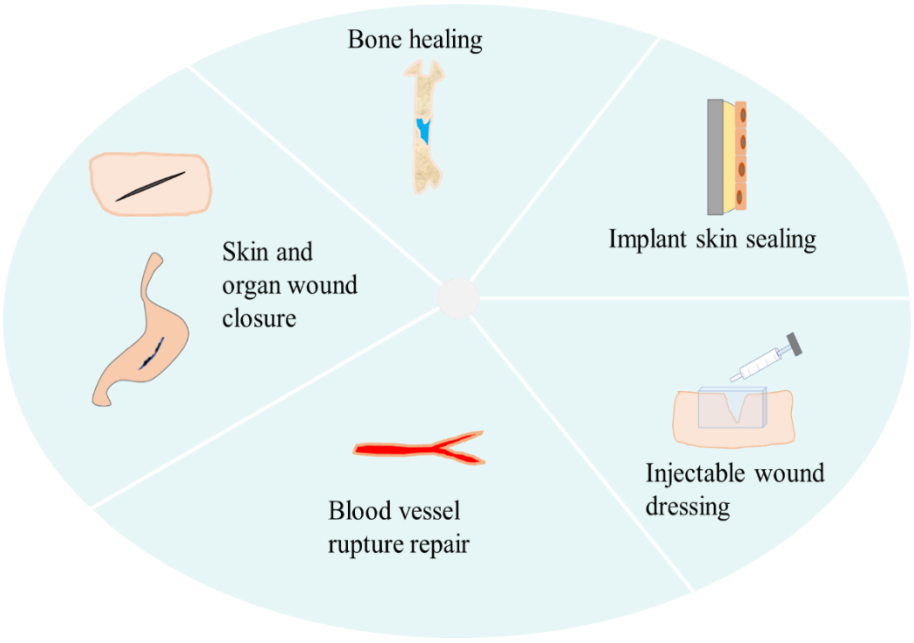

Figure 2.1: Medical applications of bioadhesive/tissue glue [40].

2.4 Commercial bioadhesives

According to bioadhesive market report of Market and Market report 2021, Bioadhesives and sealants had a market value of USD 6 billion in 2020 and is expected to reach USD 9.7 billion by 2025. These are sold under different brand names **figure 2.2**. Cyanoacrylates and the fibrin glue are most commonly commercially available glues. in fact, Cyanoacrylate adhesive was the first FDA approved bioadhesive in 1998 for human application. There are a range of commercially available cyanoacrylate adhesives used in orthopedic, neurosurgery, plastic surgery, dermatology, urology, and vascular and cardiac surgery [41]. However due to its exothermic polymerisation and also toxic degradation product release it has been replaced by some natural polymer based adhesives [42]. Fibrin glue made from human or animal plasma is better alternative as it is degraded easily with body's proteolytic enzymes, it has a combination of fibrin and thrombin that are directly injected at the site of application and allowed to settle. However, its limitations arises due to its brittle nature in aqueous environment and loss of adhesion strength due to the interference by the interfacial water layer [43]. Other polymers used for bioadhesive synthesis include Polyethylene Glycol (PEG), Poly(acrylic acid) (PAA), Poly(N-isopropylacrylamide) (PNIPAAm), etc **table 2**.

Table 2: Common commercial bioadhesives - composition and application.

Commercial/ brand name	Composition	Tissue usage
FocalSeal	Polyethylene glycol (PEG)	Pleural/lung rupture healing to prevent air leakage
DuraSeal	Polyethylene glycol (PEG)	Cranial suturing healing

Coseal	Polyethylene glycol (PEG)	Repairing blood vessel rupture
Progel	Human serum albumin (HSA)	Pleural/lung rupture healing to prevent air leakage
Tisseel	Fibrinogen and thrombin	close of surgical wound or incision
Bio glue	Bovine serum albumin (BSA) and glutaraldehyde	Maintaining haemostasis during cardiovascular surgery
Amcrylate	Iso Amyl 2-Cyanoacrylate	Bleeding control post-surgery
Enbond	n-butyl-2 Cyanoacrylate	Controlling bleeding in upper gastrointestinal tract (oesophagus, stomach, etc)
SurgiSeal	Iso Amyl 2-Cyanoacrylate	To close the surgical incision
Quickfix-Skin glue	n-Butyl-2-Cyanoacrylate	Skin wound closure

Figure 2.2: Common commercial brands of bioadhesive used in medicine.

2.5 Natural polymer based bioadhesives

A shift towards biological polymers for bioadhesive fabrication is been observed due to higher biocompatibility. Commonly used biopolymers are the polysaccharides like Alginate[44], Agarose[45], Chitosan[46], Dextrans[47], etc. Among protein fibrin has been most successful and still dominates the bioadhesive market as discussed in section , other proteins like albumin[48], collagen [49], gelatin [50] etc. other biopolymers like DNA though lesser used also has been tested for bioadhesion[51]. Though these natural polymers lack the mechanical strength of the synthetic ones combining with some crosslinker can provide better results [52].

2.6 Keratin protein for bioadhesives

Keratin protein is found in skin, hairs, horns, nails and can be easily extracted in great yield using simple procedures. A huge quantity is produced as a waste material from the slaughter houses saloons, . use of keratin could serve a bigger purpose to use the waste to create wealth for betterment of society. In addition, it can be also derived from the human sources thus minimizing the allergy chances. Other major

reasons for increased focus of biomaterial research on keratin is higher cysteine content which can be easily crosslinked in a numerous way to produce an array of biomaterials as sponge, sheet, hydrogels [53].

2.7 Keratin availability

Keratin protein is a water insoluble protein belonging to the intermediate filament protein family and is found in very large amount in various animal structures like the hoof, nails, hairs, skin, horns, etc. In fact, it is the third most widely available protein in nature only after cellulose and chitin. It is easily and cheaply available as a waste from leather industry, poultry, slaughterhouses in form of hide, feathers, hairs, etc. The percentage of keratin waste materials produced from these industries is given in **figure 2.3.** More than 40 million tons of keratin waste is produced annually worldwide, 0.2 million tons of hairs, 0.56 tons of wools, textile industry produces 2.5 million tons of keratin waste, poultry produces around 8 million tons [54]. Such a huge keratin waste is a very big problem due to its highly stable nature which deters easy degradation, has very low solubility in water and other solvents. These features are attributed to its high cysteine amino acid (7-13%) which forms disulphide bonds [55]. Thus, these persist in environment content as solid waste and clogs the drains, can be eaten up by the cattle and cause health hazards, moreover poultry feathers have a lot of infectious pathogens which can spread diseases like chlorosis and fowl cholera [56]. General methods for dealing with such a huge waste are incinerating, dumping, burning, etc. all of which leave some side effects on the environment. Thus, using keratin will in turn simultaneously help to reduce these animal wastes. It shows high biocompatibility to human tissues and being an epidermal protein, it is particularly helpful for skin-based applications like wound healing, or incision or to stop bleeding, besides there have also been many reports of using the patient's own hair as a source for the keratin (autologous). This further diminishes any chance of an immunological reaction. Keratin materials

support cell attachment and proliferation as it is highly rich in cell binding sequence LDV (Leu-Asp-Val), which easily recognize the integrins and can interact with the cell. The porous structure also helps in cell attachment and culturing.

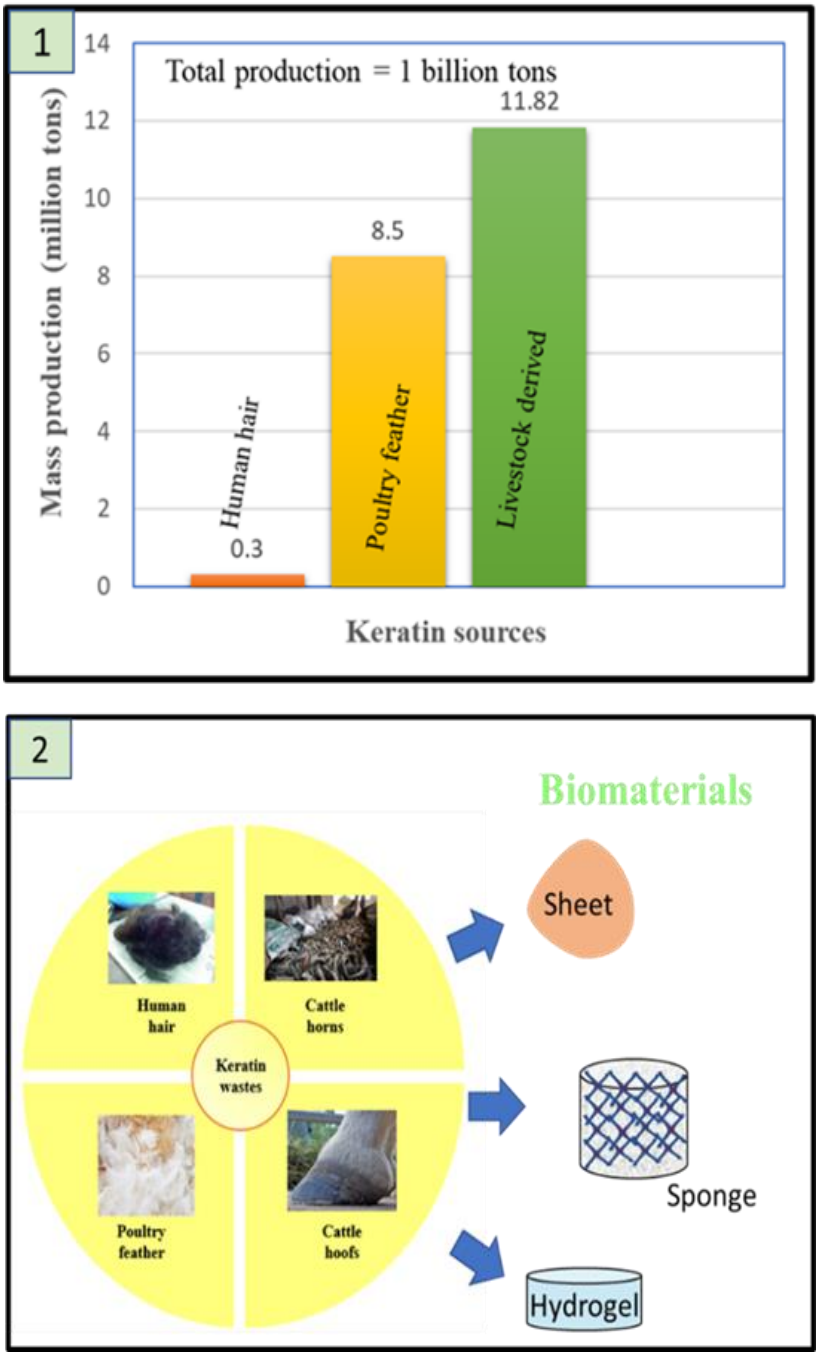

Figure 2.3: (1) Keratin from different waste material annual production [54], (2) Different biomaterials usually fabricated using keratin.

2.8 Keratin protein in animal world

Keratin is term that covers a group of protein rather than being a single protein found in the epithelial cells of the vertebrates and their modifications like horns, claws and hooves, hairs , feathers, etc. generally it has an alpha helical conformation while beta keratin is seen in Reptiles and Aves (bird) This is quite abundant protein making it 3rd most abundant protein in a mammalian body only after collagen and chitin. Being a fibrous structural protein, its major function is to maintains the structural integrity of the cells and tissues and to protective barrier against physical stress, mechanical damage, and environmental factors. In the skin, keratin constitute around 70 – 80 % of its outermost layer or stratum corneum and helps to prevent dehydration and from harmful UV radiation impacts [57]. External hard cornified structures likes, nails feathers are excessively rich in keratin (90 -95%) and responsible for their hardness and protection against external Such functional diversity in keratin is majorly due to its genetic diversity, in humans alone there are 54 known functional keratin genes in humans, also based on presence in the different tissue types could be further divided into subfamilies. Keratin location in the animal body also affects its composition particularly the cysteine content. Keratin with a higher cysteine content (10 – 20 %) also known as Hard keratin due to their compact, twisted nature produced by disulphide bonds found in structures as feathers, beaks ,etc. while soft keratin provides flexibility, elasticity, and tensile strength to the tissues it is present in. It is less resistant to mechanical stress and wears down more easily than hard keratin it is common in epithelial cells, hair etc.

2.9 Human keratin protein

Humans have around 54 keratin genes, which are distributed in epithelial skin, hair, and nail tissues. These genes are located on the chromosomes-7 and 12. Out of these 28 are of type I and rest are type II. the subfamilies KRT1-KRT8 for epithelial keratins, KRT9-KRT20

for hair keratins, and KRT31-KRT40 for keratins expressed in specific epithelial tissues **table 3**. Naming of these genes is composed of KRT (for keratin) and a number indicating specific gene within the keratin gene family [58].

Table 3: Different keratin types found in different human/ animal tissues [58].

Keratin type	Nature	Found in
KRT 1	Type II	Epithelium
KRT 2	Type II	Epithelium
KRT 3	Type II	Epithelium
KRT 4	Type II	Epithelium
KRT 5	Type II	Epithelium
KRT 6	Type II	Epithelium
KRT 7	Type II	Epithelium
KRT 8	Type II	Epithelium
KRT 9	Type I	Epithelium
KRT 10	Type I	Epithelium
KRT 11	Type I	Epithelium
KRT 12	Type I	Epithelium
KRT 13	Type I	Epithelium
KRT 14	Type I	Epithelium
KRT 15	Type I	Epithelium
KRT 16	Type I	Epithelium
KRT 17	Type I	Epithelium
KRT 18	Type I	Epithelium
KRT 19	Type I	Epithelium
KRT 20	Type I	Epithelium
KRT 25	Type I	Hair
KRT 26	Type I	Hair
KRT 27	Type I	Hair
KRT 28	Type I	Hair

KRT 71	Type II	Hair
KRT 72	Type II	Hair
KRT 73	Type II	Hair
KRT 74	Type II	Hair
KRT 75	Type II	Hair
KRT 31	Type I	Hair
KRT 32	Type I	Hair
KRT 33	Type I	Hair
KRT 34	Type I	Hair
KRT 35	Type I	Hair
KRT 36	Type I	Hair
KRT 37	Type I	Hair
KRT 38	Type I	Hair
KRT 39	Type I	Hair
KRT 40	Type I	Hair
KRT 79	Type II	Hair
KRT 80	Type II	Hair
KRT 81	Type II	Hair
KRT 82	Type II	Hair
KRT 83	Type II	Hair
KRT 84	Type II	Hair
KRT 85	Type II	Hair
KRT 86	Type II	Hair

2.10 Human hair

The human hair arises from beneath the skin surface forming hair root and has an external shaft portion. have a bulb at its base it is connected to blood vessels hair papilla and nerve ending for sensations purposes. It is the bulb portion of the hair root from where new cells are constantly made. These cells stick together and harden to give rise to strand of hair. Family consists of 17 members (**table 3**). They can be divided into two groups: acidic (or type I) group and basic (or type II) group. The acidic keratin group contains 11 members while basic ones form the 6 members.

2.11 Human hair keratin based bioadhesive

Human hair have a high keratin percentage combined with the ease of keratin extraction and least chances of the immune reaction which if any could further be reduced by using the autologous human keratin source human hair keratin has shown good results when the biomaterials derived for then many previous reported have used it as, Tamer et al. [59] Prepared a liver tissue haemostat sealant for the rat liver injury and found it to be performing better when compared to. Keratin could also be used in combination with other proteins like fibrins to enhance their injectability Hyeeon et. al. developed a conjugated keratin fibrin hydrogel that showed improved injectability and sped up the oral wound healing process [60]. Similarly, S. Thirupathi Kumara Raja et. al. by a combination of the gelatin and keratin and when used for the incision wound closure on the mouse model showed better results as healing [61].

Chapter 3
Materials and Methods

3.1 Materials

Human hair was obtained from IIT Indore male saloon, Acrylamide, Bis-acrylamide, Tetramethylethylenediamine (TEMED), Ammonium persulfate (APS), Glycine, Protein ladder, Urea, Sodium dodecyl sulphate (SDS), β-Mercaptoethanol, Tris-base, Sodium sulphide, Sodium hydroxide, Bradford reagent, Methanol, Potassium phosphate dibasic , potassium phosphate monobasic, Ellman's reagent, Tris base, Sodium chloride, Sodium hydrogen phosphate, Disodium hydrogen phosphate, Quercetin dihydrate, Paraformaldehyde, DMEM were purchased from the Hi-Media pvt. Ltd. (India); Dopamine hydrochloride and Dialysis membrane (cellulose tubing membrane MWC.O.- 14 kDa), Polycaprolactone (PCL) were purchased from Sigma Aldrich (United States). Comassine brilliant blue was purchased from SRL chemicals pvt. Ltd. (India), Whatman 1 filter paper was purchased from Cytiva (United States), Commercially pure titanium sheets (grade 2) were purchased from Metline Industries, Mumbai.

3.2 Methods

3.2.1 Extraction of human hair keratin

Hair samples were collected from the salon at IIT Indore campus, without any consideration for factors such as age, race, or ethnicity. The collected hair underwent a thorough cleaning process, which involved washing it with tap water to remove external dust, followed by three rounds of shampooing. Subsequently, the hair was dried and immersed in a delipidizing solution consisting of a mixture of chloroform and methanol in a ratio of 2:1. This delipidizing process aimed to eliminate any external oils and fats from the hair and lasted for 24 hours at room temperature. Afterward, the hair was rinsed with

water to remove any excess solvent and dried in an oven set at 60°C for a duration of 12 hours. The dried hair samples were cut into smaller pieces, approximately 1 cm in length, to facilitate the extraction of keratin. Two different chemical methods were employed for keratin extraction: oxidation-based and reduction-based strategies. In reduction method, the hair keratin was extracted using a solution consisting of 7M Urea, 0.208 M SDS, and 6% (v/v) β-Mercaptoethanol. This extraction process was carried out at 60°C for 6 hours [62]. Alternatively, a solution containing 0.125 M Na2S was used for keratin extraction, and the process was conducted for 4 hours at 40°C using a magnetic stirrer to ensure uniform mixing [63]. Once the hair completely dissolved in the extraction solution, the hair remnants were removed, and the solution was filtered using Whatman filter paper to eliminate fine solid impurities, such as small hair pieces. The resulting supernatant was then subjected to centrifugation at 700 rpm for 15 minutes at 4°C to remove residual impurities. The supernatant, containing the extracted keratin, was collected, and transferred to a dialysis membrane tube with a molecular weight cut-off (MW.C. O- 14 kDa). The dialysis process was performed at 4°C with continuous stirring using a magnetic stirrer, and distilled water was regularly changed to remove excess salts from the solution. This dialysis procedure lasted for 2-3 days. After dialysis, the hair keratin solution was freeze-dried (lyophilized) and stored at -20°C for further use. The quantification of keratin was performed using the Bradford assay, measuring the absorbance at 595 nm. A schematic representation of the hair keratin extraction process is depicted in **figure 3.1.**

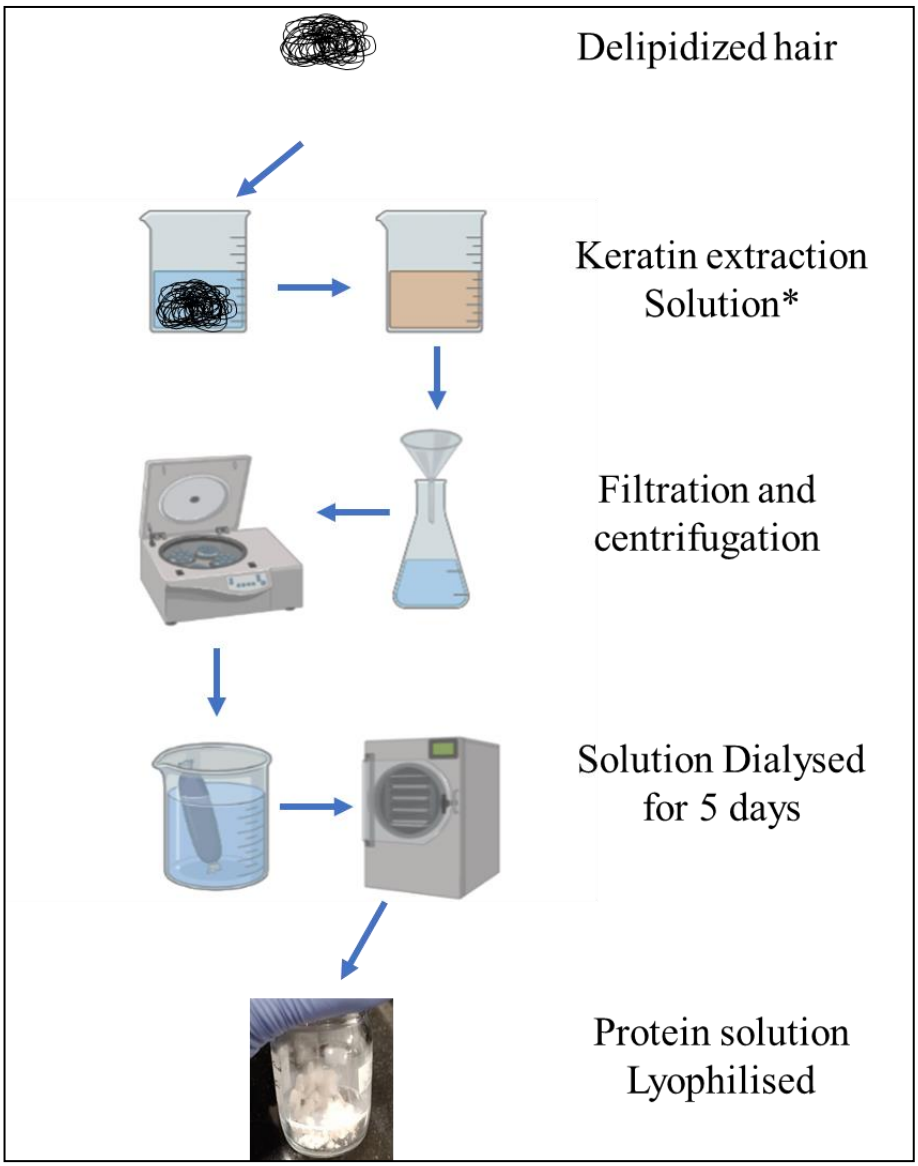

Figure 3.1: Keratin extraction mechanism from human hair [figure made from Biorender]

3.2.2 Sodium Dodecyl Sulphate - Polyacrylamide Gel Electrophoresis (SDS -PAGE)

SDS-PAGE was used to determine the molecular weight of hair keratin using the Bio-Rad Mini-PROTEAN Tetra Vertical Electrophoresis Cell. To determine the molecular weight of extracted keratin, a 12% SDS PAGE gel was prepared. After adding 4X loading buffer to the samples, they were heated to 95 °C for 10 minutes before being loaded into wells of the 12% resolving gels. It was initially run at 70 V for stacking the protein bands to the same level, then at 90 V for resolving. The movement of the tracking dye tracked the sample migration in the gel. Following electrophoresis, the gels were stained for overnight in staining solution. After staining, gel was transfer into the destaining solution for 10 to 12 hours for visualization of bands.

3.2.3 CD spectroscopy

The secondary structure of the extracted keratin was analyzed using the JASCO -2200 spectropolarimeter at 25°C using franco multipurpose cuvette. The samples were prepared by dissolving the lyophilized keratin protein in milli-Q water to get final concentration of keratin at 0.1 mg/ml. The CD spectrum (θ) of keratin solution was recorded from 190 to 260 nm at the scan rate of 50 nm/min. All the parameters such as band width, response, and data pitch were used in standard settings. The molar ellipticity $[\Psi]_\lambda$ was calculated using the formula mentioned below:

$$[\Psi]_\lambda = [\theta/100]\times C\times \ell$$

Where, θ is observed ellipticity, C is the concentration of sample in g/ml and ℓ is the cell path length in cm [64].

3.2.4 FTIR Spectroscopy

FTIR spectra of the extracted keratin sample was recorded using the Agilent Technologies Cary 630 FTIR spectrometer equipped with diamond crystal. It was operated in the attenuated total reflection (ATR) mode. All samples were scanned between 4000–500 cm^{-1} at a resolution of 4 cm^{-1}. All the readings were reported as an average of 62 scan and at room temperature.

3.2.5 Free thiol group content in extracted protein

The level of free thiol groups in a protein sample containing keratin was determined using Ellman's reagent, also known as 5,5'-dithiobis (2-nitrobenzoic acid) (DTNB). The Ellman's reagent was prepared by dissolving 0.3 mg/ml of DTNB in a phosphate buffer with (0.5 M) and a pH of 8. A standard solution was prepared using a cysteine solution. The extracted hair keratin (1 mg/ml) was added to the Ellman's solution. The reaction between the protein sample and the reagent was allowed to proceed for 2 hours at room temperature (RT), and the absorbance of the resulting solution was measured at a wavelength of 420 nm [65].

3.2.6 Hydrogel preparation using the Human Hair Keratin

Hydrogels were prepared using a combination of chemical and physical crosslinking methods. In the chemical crosslinking approach, different concentrations of polyphenol crosslinkers, specifically Dopamine and Quercetin, were utilized. Varying mass ratios (m/m) of the protein to polyphenol were employed to observe the impact of concentration on gel crosslinking, as detailed in Table 2. The total volume of all solutions was maintained at a constant 2 ml. To accelerate the gelation process, physical crosslinking was employed through the freeze-thaw method. This involved placing the keratin-polyphenol

solution in a -20°C refrigerator for an extended period until it completely froze, followed by thawing at 4°C for 20 minutes. The gelation was assessed using tests such as tube inversion or tube tilt to determine the formation of a gel-like consistency.

Table 4: : Different weight ratios of hair keratin protein: polyphenol used to prepare hydrogels.

Extracted keratin : Polyphenols ratio		Total volume (ml)
1	1	2
2	1	2
5	1	2
10	1	2

3.3 Hydrogel characterization

3.3.1 Swelling behaviour of hydrogels

The measurement of water content in the hydrogel was conducted using the following procedure. Initially, the prepared hydrogels were left at room temperature for an extended period of 4 hours to allow any excess water to evaporate. If necessary, a kim wipe was used to wipe away any remaining moisture, resulting in the hydrogel reaching its fully hydrated equilibrium state. The weight of the hydrogel was then measured at this point. Subsequently, all the water trapped within the porous matrix structure of the hydrogel was extracted by subjecting it to lyophilization for 12 hours [66]. This process transformed the hydrogel into a porous scaffold or aerogel, and its weight at this stage was referred to as the dry weight of the hydrogel. Water content was measured using below **equation 1**.

$$\text{Water content (\%)} = \left(\frac{y-x}{x}\right) * 100$$

x mass of dried scaffold
y mass of hydrogel

…eq. 1

3.3.2 Microstructure of the hydrogels

The surface morphology of the hydrogels, including the crosslinking density of protein filaments, microporous structure, and pore sizes, was examined using Scanning Electron Microscopy (SEM). To begin with, the hydrogels underwent the same lyophilization process described in section 3.3.1. Subsequently, the lyophilized hydrogels were coated with a thin layer of gold using the EMS150T ES turbo-pumped sputter coating machine for a duration of 1 minute. This gold coating served to enhance the conductivity of the samples. The microstructure of the hydrogel was then observed using a JEOL - JSM-7610F Plus SEM machine at two different magnifications (**300X and 500X**).

3.3.3 Rheological features of hydrogels

Rheological measurements of the hair keratin dopamine and hair keratin quercetin hydrogels were carried out using an Anton Paar Physica MCR 301 Rheometer. The rheometer was set up in a parallel plate arrangement, with a plate diameter of 25 mm. A small piece of the hydrogel sample was cut and placed on the lower plate of the rheometer, and the upper plate was brought closer to maintain a 1 mm gap between the plates. Prior to taking measurements, the rheometer was calibrated for 5 minutes in the same arrangement. To determine the linear viscoelastic region (LVER) of the hydrogels, an amplitude sweep experiment was performed. This involved applying a constant angular frequency of 10 rad/s while varying the stress from 1 to 1000 Hz. The LVER was identified based on the behaviour observed during this experiment. Subsequently, a frequency sweep was carried out within

the previously determined LVER, using a controlled strain rate of 1%. The angular frequency was varied from 10 to 100 rad/s during this measurement. To investigate the flow rate and viscosity changes of the hydrogels, as well as their thixotropic nature, a thixotropic analysis was performed. This analysis aimed to study the variations in viscosity under different shear strain rates ranging from 1 to 100 rads/s. The thixotropic properties, specifically the reversible sol-gel behaviour in response to applied stress, were examined through cyclic strain experiments. These experiments were conducted at a constant frequency of 10 rad/s [67], while the applied strains were varied from 1 to 100%. Each deformation was applied for a duration of 3 minutes, followed by a 3-minute relaxation period. This cycle was repeated four times. After the fourth cycle, the recovery percentage was calculated to determine the extent of recovery or restoration of the original state of the hydrogels. This measurement provided insights into the thixotropic behaviour and the ability of the hydrogels to revert back to their initial state after undergoing stress-induced changes.

3.3.4 Injectability of the hydrogels

To demonstrate the viscoelasticity and thixotropy of the hydrogels, an injectability test was performed. The hydrogels were loaded into a 10 ml syringe (without a needle) and injected into a beaker that was half-filled with water. This was achieved by slowly pressing the handle of the syringe to dispense the hydrogel material. To visually distinguish between the hydrogel's, different coloured dyes were added to each. Congo Red dye was used for the hair keratin-dopamine gel, resulting in a red color, while Trypan Blue dye was used for the hair keratin-quercetin gel, giving it a blue color. This coloration helped differentiate between the two hydrogel formulations during the injectability test. Furthermore, the ability of the hydrogels to be extruded into fine fibres, a property important for their application in 3D bioprinting as ink, was assessed. This was achieved by using the same syringe setup to draw an

arbitrary shape on a glass plate, allowing the hydrogel to be dispensed in a controlled manner to form the desired pattern or structure [67]. By performing these injectability and fibre extrusion tests, the viscoelastic and thixotropic properties of the hydrogels could be observed and evaluated, demonstrating their potential application in various biomedical fields.

3.3.6 Adhesive properties of hydrogels

The adhesion behaviour of the hydrogel was qualitatively demonstrated through a series of basic tests. Firstly, the hydrogels were affixed to a titanium (Ti) sheet and then inverted to observe their ability to stick to the titanium implant surface. To assess adhesion to the skin matrix, a substitute for the skin was used in the form of a polycaprolactone (PCL) membrane. This membrane was electro spun using e-Spin technology. The hydrogel was applied to the PCL membrane to examine its adhesion behaviour to a skin-like surface [68]. To analyze the simultaneous binding of the hydrogel to both the skin substitute and the implant, a sandwich structure was created. The hydrogel was placed between the Ti sheet and the PCL membrane, and Ti sheets of varying weights (2g, 3.7g, and 6.3g) were used to quantify the strength of adhesion. By lifting the Ti sheets, the force required to detach the hydrogel from the combined skin and implant model was measured. Through these tests, the qualitative adhesion behaviour of the hydrogel was evaluated in terms of its affinity towards the titanium implant, its adhesion to a skin substitute, and its ability to simultaneously bind to both the skin matrix and the implant surface.

Chapter 4

Results and Discussions

4.1 Keratin extraction

Keratin was extracted from human hair under relatively milder conditions unlike the harsh treatment needed for animal sources like hoofs, horns, etc. Keratin from hair is a significant source along with other sources of keratin and extracting keratin from human hair protects the native structure of keratin. Keratin was extracted from human hair based on reduction method. Among different methods used for keratin extraction such as steam explosion [69], thermal hydrolysis [70] microwave irradiation [71], enzymatic treatment [72], chemical hydrolysis using some chemical agents is the most common method due to ease and simple instrumentation [73]. Method used for extraction of keratin based on chemical hydrolysis are of two types: reduction and oxidation-based method. Reduction based method breaks the disulphide bond in protein to form a free sulfhydryl group generating reduced form of keratin. The optimum pH range required for extraction was 6-8, as keratin neither extracted at acidic pH and nor at alkaline pH. Commonly used method, reduction-based method also called Shindai solution, a well-established method by Nakamura et al. [74], sodium sulphide method [75], thioglycolic acid method [76].

In this thesis, extraction of keratin was done using two different methods. First one is sodium sulphide method, utilizes 0.125M sodium sulphide which acts as reducing agent. The second method for keratin extraction involves the use of urea (to break noncovalent bonds), SDS (for disruption of strong intermolecular interaction), and β-mercaptoethanol (to cleave the disulphide bond in keratin) at 60℃. The solution is expected to be stable for a period when stored at ambient temperature of -20℃. Further the concentration of hair keratin extracted can be estimated by Bradford assay and the obtained concentration of keratin was 21.8 mg/ml from by the urea-based method and 14 mg/ml

by the sodium sulphide method. The calculated efficiency of these two methods was found to be 21.68 % and 12 % respectively shown in **figure 4.1.**

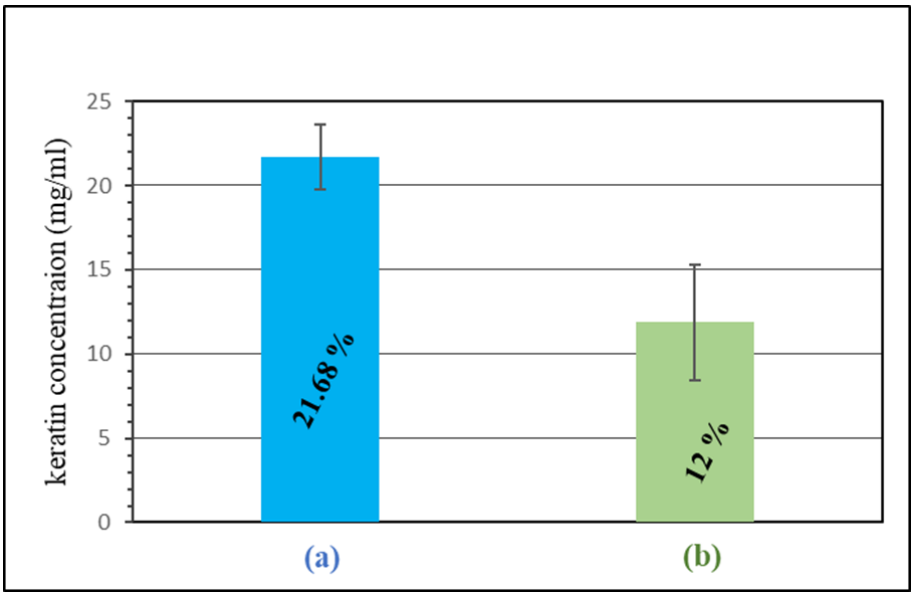

Figure 4.1: Yield efficiency of keratin extraction methods: (a) 7 M Urea + 0.208 M SDS + (6 % v/v) β-mercaptoethanol (6 h) (b) 0.125 M Na_2S (4 h).

4.2 Sodium Dodecyl Sulphate - Polyacrylamide Gel Electrophoresis (SDS PAGE)

SDS- PAGE of extracted keratin **figure 4.2** showed two distinct bands of around 60 kDa and 40 kDa size using 12% polyacrylamide gel, which is in accordance with already reported data was showed in figure 4.2(i). Human hair is rich in keratin protein (approximately 95%) and most of it is in the cortex layer of hair follicle that forms the middle portion of hair cross-section. This keratin exhibits the helical secondary structure with two different alpha helices coiled to form a coiled coil dimer, one of these helices belong to type I (acidic, M.W- 40 kDa) keratin and other type II (basic, M.W- 60 kDa). Out of the total 17 types of keratins found in hair, 11 are type I while 6 are type II, and only compatible helixes pair with each other and it is shown in **figure 4.3**. These dimers then act as a repeating unit to form a tetramer, octamer

etc. in alternating manner till a 10 nm thick fibre is achieved, also called intermediate filament [77]. The other layers of hair cross-section include an outermost cuticle made of flat, dead overlapping cells giving a scaly appearance under microscope, while innermost layer is simply composed of hollow spaces along with some packed cells. There is yet another minor class of proteins in the hair shaft called as γ-keratin or the keratin associated protein (KAP), these represent numerous short proteins of M.W- 10 kDa to 40 kDa range. Their main function is to create an interfilamentous matrix holding on the different keratin filaments by disulphide bonds [78].

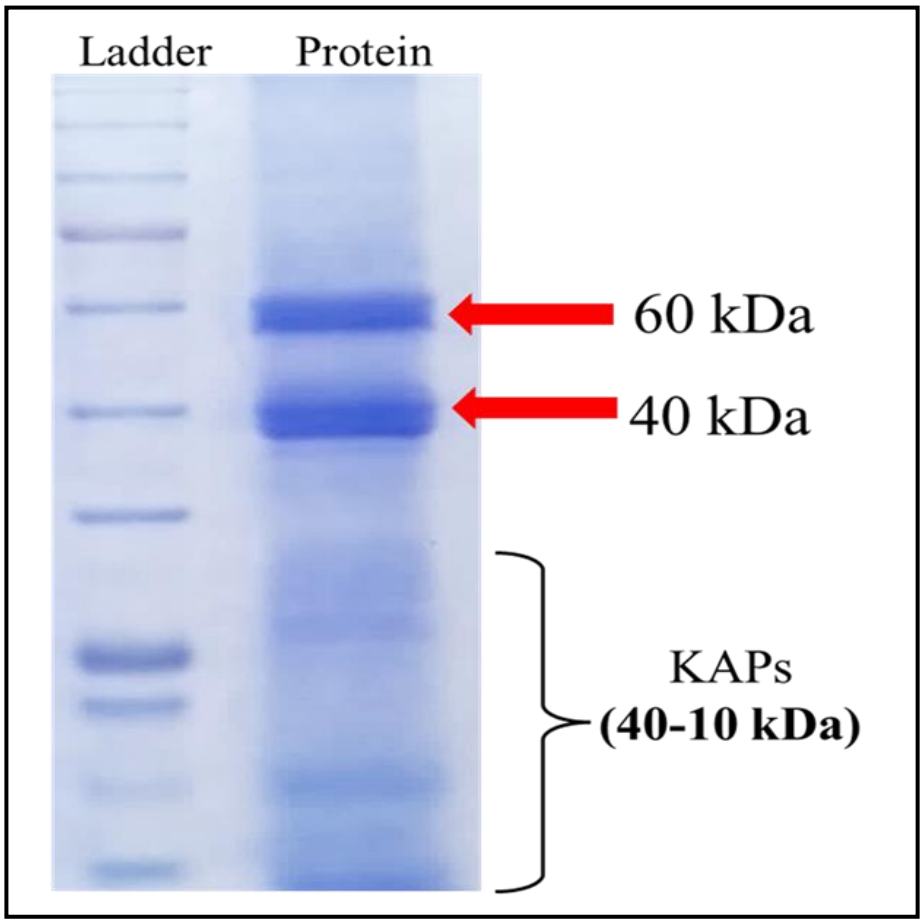

Figure 4.2: (i) SDS-PAGE showing two distinct bands of appropriate size for extracted keratin. Additionally, few bands of keratin associated proteins (KAPs) required for helical folding of keratin are visible.

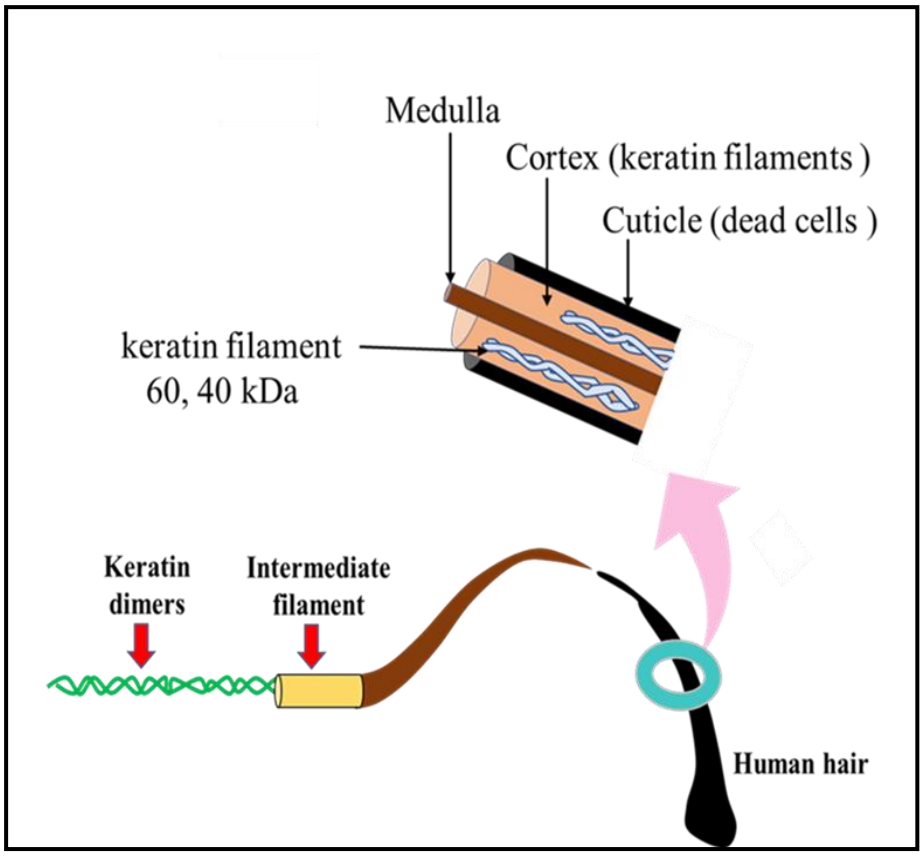

Figure 4.3 Hair structure in a cross section though its shaft showing different layers - cuticle, cortex, and medulla from outside to inside [77].

4.3 Circular dichroism (CD) Spectrum of Keratin

CD is a spectroscopy technique that measures the absorption difference between left and right circularly plan polarized light. It's a technique to elucidate the secondary structure of protein due to presence of several chiral centres/asymmetric centres in the amino acid side groups and the central carbon atoms in all the amino acids except for glycine. These chiral centres differentially absorb a circularly polarised light (i.e., unequal absorption of left-handed and right-handed circularly polarized light). Depending on the absorbed wavelength and the distinct peaks implies the kind of secondary structure (α-helix, β-sheet, or random coil etc.) present in the protein by comparing with the standards. Briefly, α-helical proteins have negative bands at 222 nm and 208 nm and a positive band at 193 nm. Proteins with well-defined antiparallel β-pleated sheets (β-helices) have negative bands at 220 nm and positive bands at 190 nm, while disordered proteins (random coil) have very low ellipticity above 210 nm and negative bands near 195 nm [79]. In case of human hair keratin (as shown in **figure 4.4**), the CD spectrum showed two negative bands at 220 nm and 210 nm also a positive band was seen around 190 nm. Indicating that hair keratin adopts predominantly α-helical conformation. Hair keratin is composed of the helical keratin protein discussed in section 2.5. This is in conformation with the available data reporting the keratin to be primarily a helical protein. Hence, CD confirms that the extracted keratin contains ordered structure and is not in denatured form.

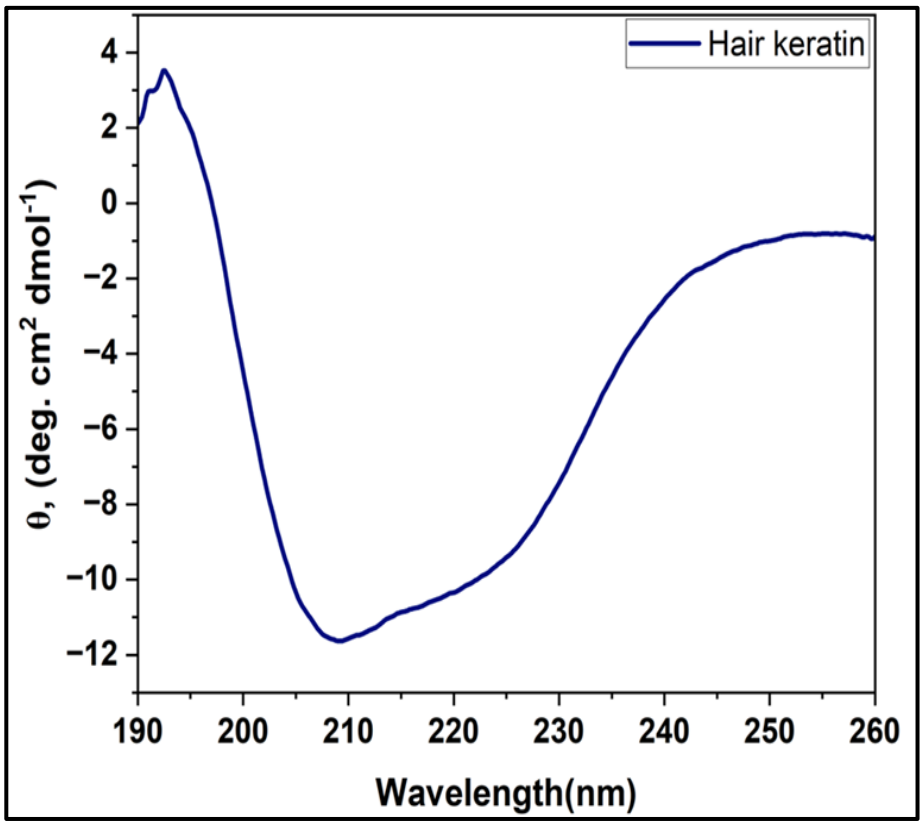

Figure 4.4: CD spectrum of the human hair keratin, two negative peaks observed at 210 nm and 219 nm followed by a positive peak at 195nm.

4.4 Fourier-transform infrared spectroscopy (FTIR) spectrum of protein

FTIR spectroscopy was also used to investigate the secondary structure of keratin. FTIR, is an IR spectroscopy method and used to analyse the functional groups and molecules by their vibrations (stretching and bending) upon absorbing the IR light (wavelength range 700-4000 nm). FTIR produces different characteristic peaks for different types of molecules like protein which have amide bond as the most characteristic bonds. Proteins show different amide peaks as the amide I, amide II, amide III, and amide A their corresponding wavenumber range given below in **table 5**. Some of the characteristic peaks obtained in FTIR was highly sensitive to secondary structure of hair keratin such as amide I peak due to the NH bonding. Consequently, the secondary structure of hair keratin was examined in powder form. Similar to CD, FTIR exhibits characteristic bands for α-helix, β-sheet, β-turn, and random coil conformations in the amide I (1700–1600 cm^{-1}) and amide II (1560–1500 cm^{-1}) region. Among these regions, amide I (due to the C=O stretch vibrations of the peptide linkage) is more sensitive to protein secondary structures. It is well established that α-helical conformation has an amide I and II (mainly from in-plane N-H bending and from the C-N stretching vibration) bands between 1657 and 1650 cm^{-1} and between 1550 and 1540 cm^{-1} , respectively, while the β-sheet has an amide I and II bands between 1635 and 1615 cm^{-1} and between 1535 and 1520 cm^{-1}, respectively. Amide III has band between 1300-1230 cm^{-1} (N-H bending and C-N stretching), another important band for protein characterization [80] The FTIR spectrum of hair keratin in lyophilized keratin is shown in **figure 4.5**. The extracted keratin shows an amide I and II bands at 1643 and 1528 cm^{-1}, respectively, which are characteristic of α-helical conformation. The FTIR result thus clearly suggests that keratin adopts predominantly α-helical conformation.

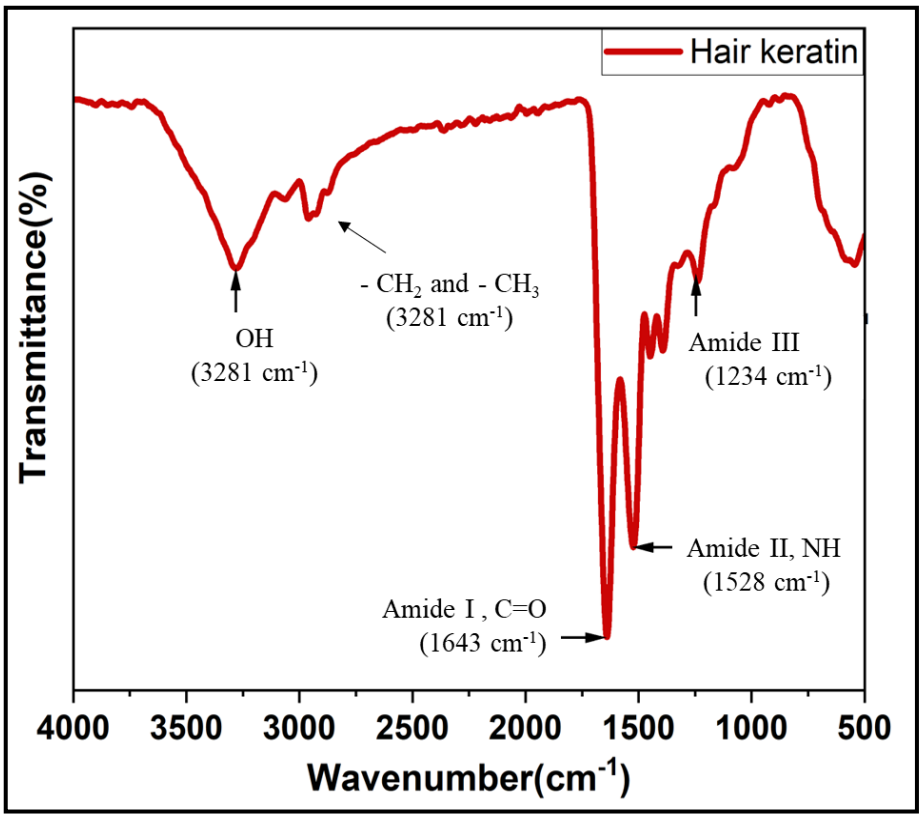

Figure 4.5: FTIR spectrum of extracted hair keratin. Amide I and II are found to be a characteristics peaks for hair keratin.

Table 5: Characteristic peaks for α – helical protein conformation studied by FTIR [80].

FTIR peak	Wavenumber (cm^{-1})	Bond vibration
Amide I	1657- 1650 cm^{-1}	C = O stretching
Amide II	1540 -1550 cm^{-1}	N-H bending, C-N stretching

4.5 Ellman's test

Sulfhydryl groups in proteins play a crucial role in protein conformation and binding due to its high ability to form disulphide bonds. Since the keratin protein has high cysteine content (approximately 10%), it is an important functional group for crosslinking of the keratin to form the hydrogel . Commonly used methods for the detection and quantification of the free -SH groups are using (5,5-dithio-bis-(2-nitrobenzoic acid) (DNTB) also called Ellman's reagent. It is a colorimetric assay where DTNB reacts with the conjugate base (R—S-) of a free sulfhydryl, oxidizing the S-H group, and reduced to a yellow coloured compound 2-nitro-5-thiobenzoic acid (TNB). TNB shows strong absorption at 412 nm, and the mechanism is illustrated in **figure 4.6**. Hence, its molar concentration can be analysed using absorbance formula A= ε.c.l, where ε- molar extinction coefficient of the TNB which is 14000 m^{-1} cm^{-1} [81]. Concentration of TNB is proportional to the number of S-H groups oxidised. Here the concentration of total thiol group present in the extracted hair keratin from urea-based method was 0.27 mM.

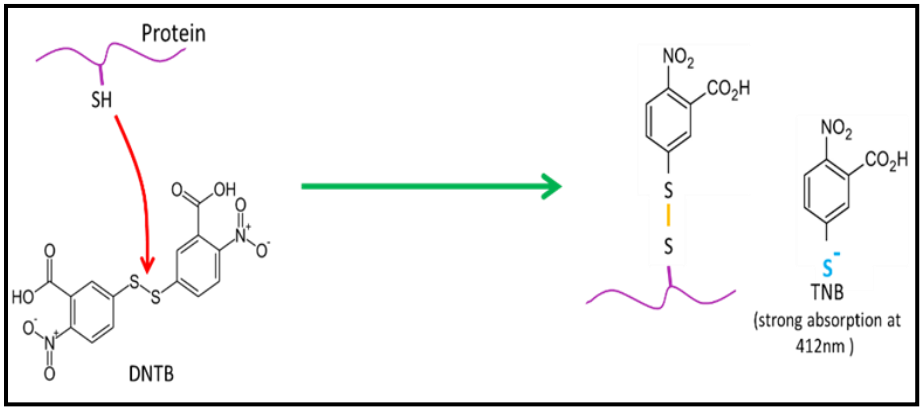

Figure 4.6: Schematic representation of the Ellman's reaction for detection of free thiol groups.

4.6 Hydrogel preparation

Hydrogel from human hair keratin was prepared using a combination of two mechanisms – chemical crosslinking and the physical crosslinking, Michael addition crosslinking using polyphenols (Dopamine, Quercetin with a number of catechol groups) and the other is the physical crosslinking of the protein directly by freezing it completely to facilitate the disulphide bond formation between the chains. The polyphenols quercetin and the dopamine have the catechol groups which upon autoxidation gets converted to the quinone form which is a strong electrophile and thus attack numerous nucleophilic groups present in the protein such as the amine ($-NH_2$), sulfhydryl groups (-SH) [82]. Since the keratin is extremely rich in the -SH groups, the contribution by them is much more. Upon using Different mass ratios of protein to polyphenol (*m/m*), hydrogels we got had different consistencies and could be visually distinguished as seen in **figure 4.7**. It was observed that with a very high polyphenol concentration (1:1), very low crosslinking was achieved and a gel with uneven consistency produced, because of the excess of the polyphenols that exceeded the amount of the free thiol groups in proteins so inspite of crosslinking the polyphenols bounded to the individual thiol groups leading to more of precipitation. With further increase in the protein content compared with the crosslinkers the gel consistency was continued to improved. And very good solid like gels were observed at the mass ratio of 10:1. However, the covalent crosslinking alone was showing a delayed gelation (around 1-4 days) to fasten the gelation physical crosslinking by the freeze thaw mechanism was used. Free thawing represents a standard protein crosslinking mechanism, upon freezing the solution of protein with crosslinker all the solvent molecules get crystallized this minimizing in the volume and hence the protein functional groups are able to come close to other and also to the crosslinker which then easily help in bond formation [83]. Hydrogel preparation was checked by tilt test or the tube inversion test. Mechanisms for chemical crosslinking by

catechol and physical freeze thaw method is shown in **figure 4.8** and **4.9** respectively.

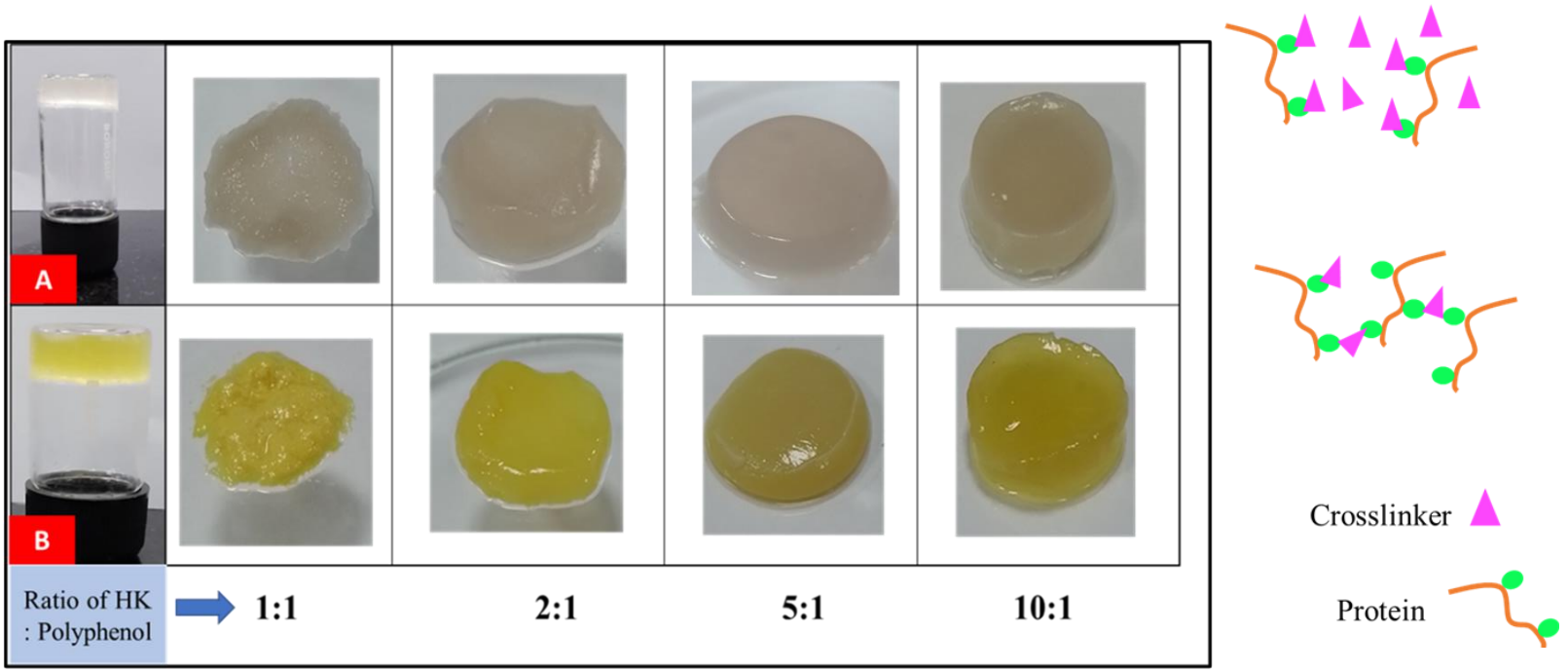

Figure 4.7: Hydrogels prepared with weight ratios (w/w) of the keratin protein: polyphenol (A) Hair Keratin: Dopamine (B) Hair Keratin: Quercetin.

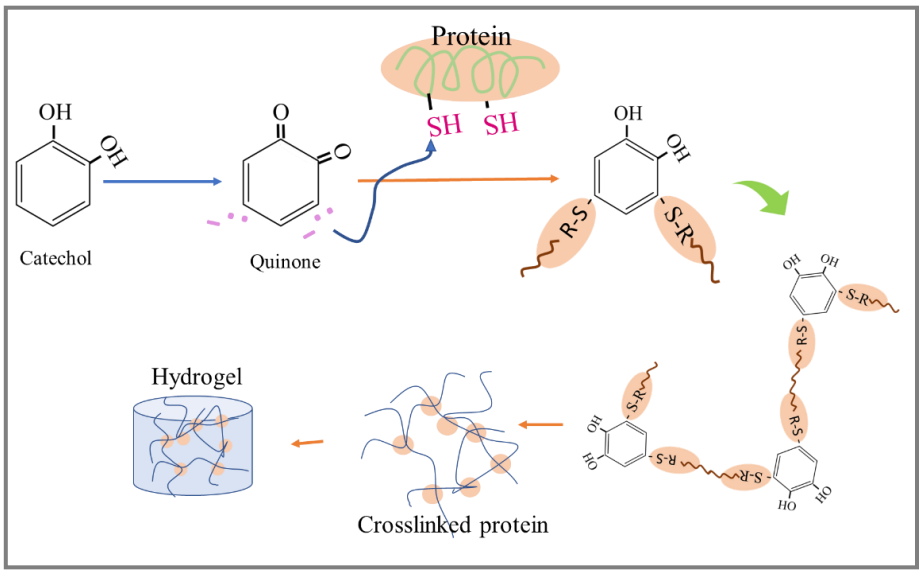

Figure 4.8: Mechanism of hydrogel preparation (Michael addition reaction). Polyphenols (dopamine and quercetin) comes in contact with keratin, it undergoes a series of oxidation reactions. The reactive catechol group present in polyphenols can react with amino acid residues, primarily cysteine, on the keratin protein. This reaction leads to the formation of covalent bonds between polyphenols and keratin, resulting in the crosslinking of the protein structure.

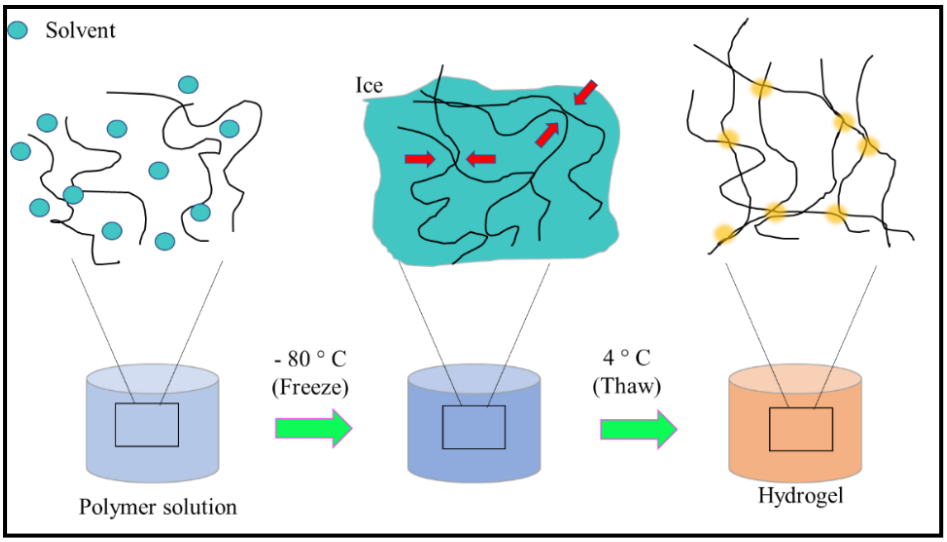

Figure 4.9: Polymer crosslinking/ gelation by freeze thaw method - upon freezing, solvent molecules undergo volume reduction and crystallization bringing the protein / crosslinker reactive groups closer to facilitate covalent bond formation.

4.7 Hydrogel characterization

4.7.1 Swelling ratio

The swelling ratio in hydrogels is a measure of how much a hydrogel can absorb and retain water or other solvents. It is a ratio that quantifies the change in volume of the hydrogel when it is exposed to a solvent compared to its original dry state [84]. Water content or swelling ratio of hair keratin dopamine and the hair keratin Quercetin hydrogel was found to be (**27.4 ± 0.3) X** and **(28.31 ± 0.8) X** respectively, X here represents the multiple times of weight of hydrogel scaffold which is water entrapped (i.e., 1 g of the dopamine hydrogel and quercetin hydrogel can hold up to 27g and 28 g of water respectively). It is inversely proportional to the polymer density and the degree of crosslinking; a higher swelling ratio is representative of more pores and less polymer density and vice versa. It is shown that higher water content for the hair keratin dopamine hydrogel represents a higher crosslinking of the protein polymers in the dopamine as compared with the quercetin, this result was later confirmed also using the SEM analysis. **Figure 4.10** illustrated the hydrogel and its corresponding scaffold post lyophilization, and the formula used to calculate swelling ratio is given as **equation 2.**

$$sweling\ ratio = \frac{x - y}{y}$$

Where, x -weight of the hydrogel, y – weight of scaffold ….eq. 2

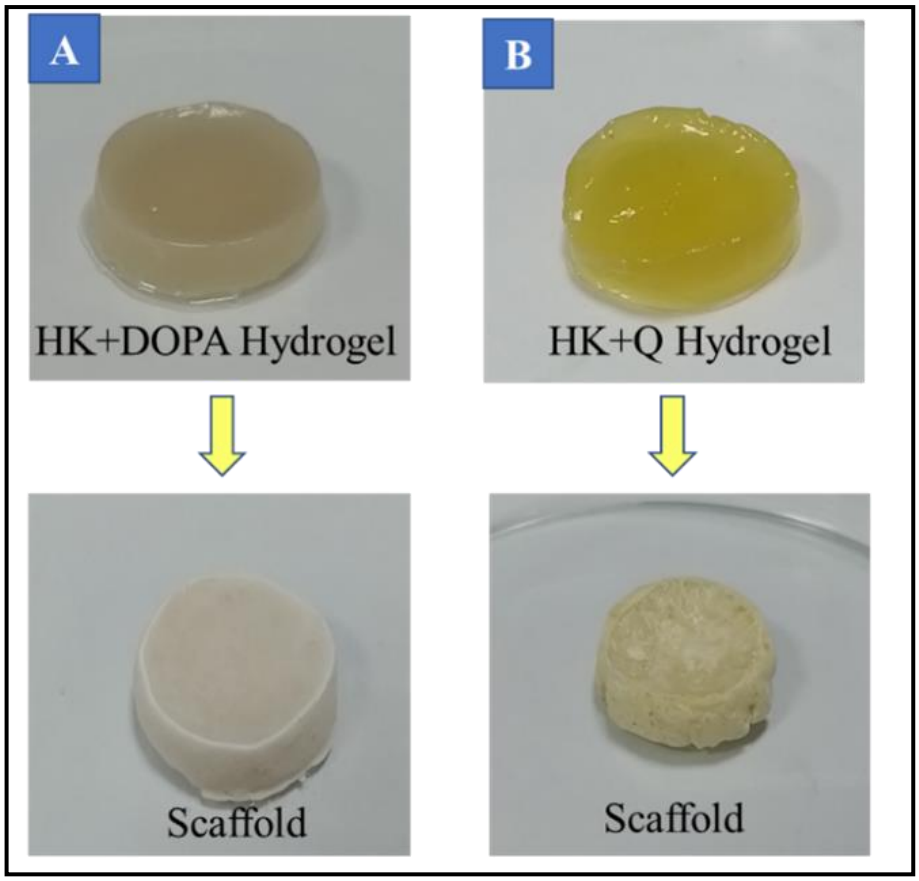

Figure 4.10: Hydrogel and its corresponding freeze dried scaffold - (A) Hair keratin dopamine (B) Hair keratin quercetin.

4.7.2 Microstructure of hydrogel

SEM microscopy was used to analyse the surface and interior morphologies of the hydrogels. Lyophilized hydrogels exhibited irregular porous structure, as shown in **figures 4.11**. The SEM images provided a glimpse into the interior structure of the hair keratin dopamine and quercetin hydrogels. The hydrogels displayed a three-dimensional (3D) network structure, often resembling interconnected pores or channels. These pores are crucial for promoting the diffusion of nutrients, oxygen, carbon dioxide, and metabolites within the hydrogel matrix. The presence of such interconnected porosity facilitates cell growth and metabolic activity, making keratin hydrogels suitable for 3D cell culture applications [85]. In our study both the

hydrogels showed the porous structure and analysed with the **Image-J Software Tool**. The pore size varied depending on the concentration of polyphenols and number of crosslinker presents Also, the dopamine seems to possess greater density of the polymers which might be due to the polymerization of dopamine into the polydopamine which leads to higher crosslinking. The size and distribution of these pores within the hydrogel matrix can vary depending on the preparation method and the concentration of keratin used. Higher keratin concentrations often result in a denser network structure with smaller pores, whereas lower concentrations may yield a more open and porous structure. Fine-tuning the concentration and processing parameters allows for tailoring the microstructure of the hydrogels to suit specific applications.

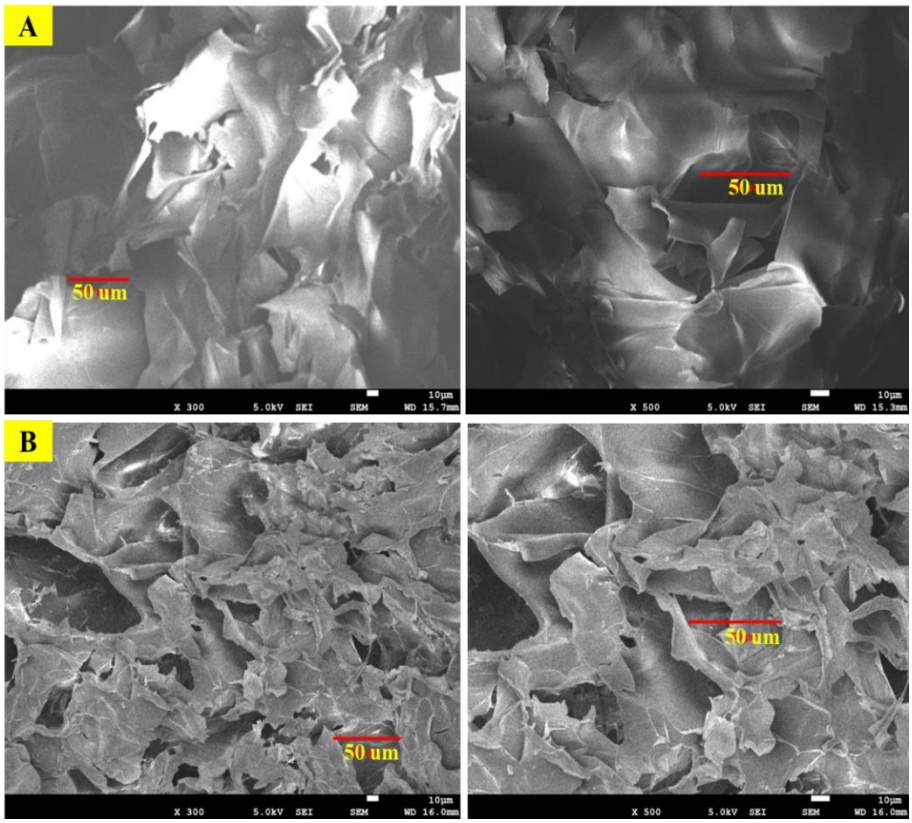

Figure 4.11: Surface morphology of the lyophilized scaffolds (A) Keratin Dopamine and (B) Keratin Quercetin.

4.7.3 Rheological analysis of hydrogels

Rheology is a valuable technique for characterizing the viscoelastic properties and shear thinning behaviour of hydrogels, as well as other thixotropic materials such as sauces, ketchup, cement, and toothpaste. It provides insights into the material's response to applied stress, including its sol-gel transition and flow behaviour. When stress is applied to a hydrogel, it undergoes a Sol-Gel transition, changing from a gel-like state to a flowing state . This transition is observed when the applied stress exceeds a certain threshold, beyond which the hydrogel starts to flow. The point at which this transition occurs is often referred to as the linear viscoelastic region (LVER). The LVER represents the stress range in which the hydrogel maintains its gel-like consistency. In rheology, two key parameters are often measured: the storage modulus (G') and the loss modulus (G"). These moduli represent the solid-like and liquid-like behaviours of the hydrogel, respectively. The storage modulus, G', quantifies the material's ability to store elastic energy when subjected to stress. It reflects the solid portion of the hydrogel and indicates its structural integrity. The loss modulus, G", measures the energy dissipation or viscosity of the material. It represents the liquid-like behaviour of the hydrogel and indicates its ability to flow under stress [86]. Both the Hair Keratin-Dopamine and quercetin hydrogels exhibit an initial storage modulus that is higher than the loss modulus shown in **figure 4.12 (1) and 4.13 (1)** respectively. This indicates a predominance of solid-like behaviour in the hydrogels. As stress is applied, the storage and loss moduli remain relatively constant up to a certain point known as the yield point. Beyond this point, with increasing stress, the fluid consistency of the hydrogel becomes more prominent. Upon comparing the amplitude sweep graphs **figure 4.12 (2) and 4.13 (2)**, it was evident that the hair keratin-Dopamine hydrogel exhibited a much higher storage modulus (G') and greater elasticity compared to the quercetin hydrogel. This can be attributed to the stronger crosslinking observed in the dopamine-based hydrogel, which forms polydopamine and provides better

crosslinking with the hair keratin compared to the quercetin hydrogel [87]. **Figure 4.12 (3) and 4.13 (3)** illustrate the shear thinning behaviour or injectability of the hydrogels, their viscoelastic changes with shear rate were examined. It was observed that both the Hair Keratin-Dopamine and quercetin hydrogels displayed an exponential decrease in viscosity as the shear rate increased. Additionally, considering the higher initial viscosity of the dopamine gels, it suggests that they possess greater injectability compared to the quercetin hydrogels. The higher initial viscosity indicates that the dopamine hydrogels are more resistant to flow under low shear conditions, making them more suitable for applications where controlled injectability is desired. Furthermore, both hydrogels demonstrated good recovery of the storage modulus after undergoing shear stress. The Hair Keratin-Dopamine hydrogel exhibited a recovery percentage of 90% in **figure 4.12 (4)** while the quercetin hydrogel showed a recovery percentage of 95% shown in **figure 4.13 (4)**. This indicates that both hydrogels have the ability to regain their original gel-like consistency after experiencing shear forces, highlighting their resilience and ability to maintain their structural integrity.

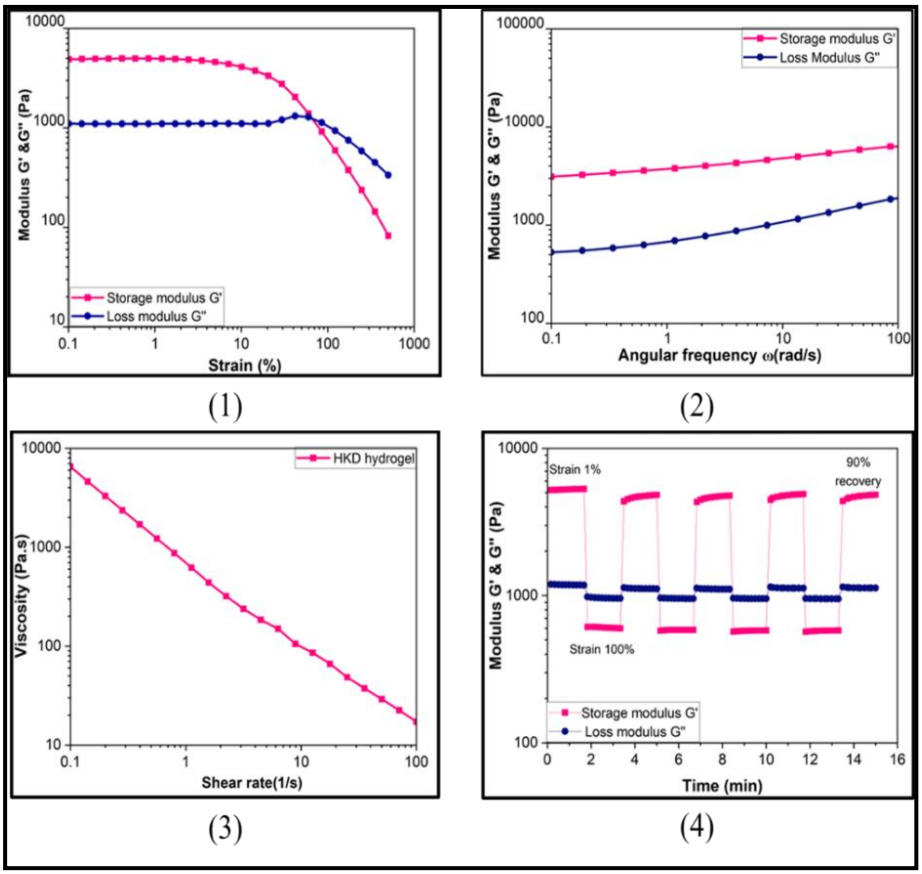

Figure 4.12: Rheological analysis of the hair keratin dopamine hydrogel (1) Amplitude sweep curve at 10 rad s -1 , (2) Frequency sweep graph at 1 % strain (3) Shear thinning behaviour of hydrogel studied through viscosity creep test (4) Cyclic strain recovery.

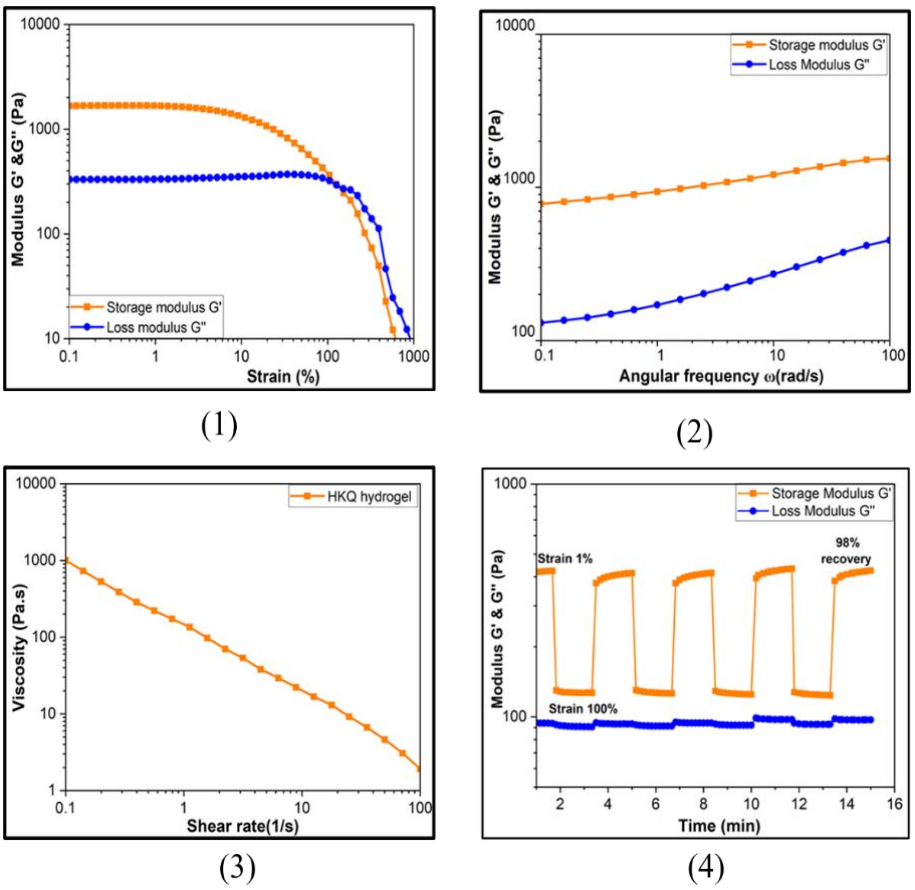

Figure 4.13: Rheological analysis of the hair keratin quercetin hydrogel (1) Amplitude sweep curve at 10 rad s -1 , (2) Frequency sweep graph at 1 % strain (3) Shear thinning behaviour of hydrogel studied through viscosity creep (4) Cyclic strain recovery.

4.7.4 FTIR of Keratin polyphenol hydrogels

For conforming the presence of the polyphenols in our hydrogels and its binding to protein polymers. FTIR peaks obtained with the lyophilised keratin was analysed and compared with that obtained with hair keratin alone and for the polyphenols alone. The strong -OH peak observed at the 3250 – 3600 cm^{-1} that represents the abundant -OH functional groups present in the catechol groups also the aromatic ring peaks which are observed in that region gives the idea of the presence of the catechol groups in the hydrogels. Their binding to free thiol groups of keratin protein by the Michael addition reaction was

confirmed by the peak representing the C-S bond peak (700 nm) was indicated in **figure 4.14 (1), (2)**.

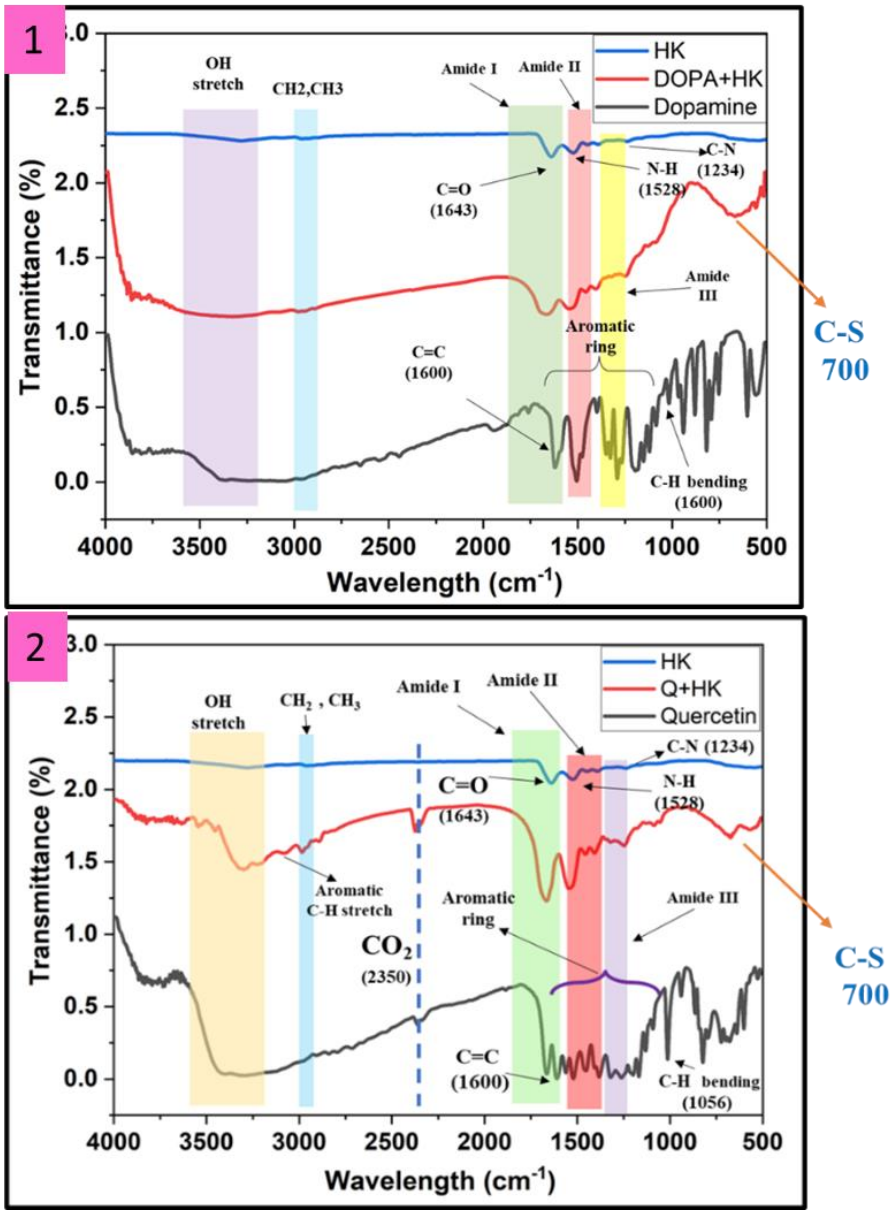

Figure 4.14: FTIR spectra to compare hydrogel crosslinking - (1) Hair keratin dopamine, (2) Hair keratin quercetin.

4.7.5 Adhesion behaviour of the hydrogels

The adhesiveness of hydrogels refers to their ability to effectively bind to different surfaces. Hydrogels with strong adhesion properties are required as tissue adhesives and glues. They are commonly employed in painless wound closure, as scaffolding material, and in reducing operating time and the need for donor tissue in organ transplants. Their binding to various inorganic and organic surfaces is facilitated by different types of bonds such as electrostatic interactions, hydrophobic interactions, Van der Waals forces, hydrogen bonding, or metal coordination [88]. Commonly used tissue glues include synthetic cyanoacrylates and fibrin glue. However, these suffer limitations as these release toxic degradation products and also lose their adhesion in the presence of water due to interference from the interfacial water layer, significantly reducing their adhesive strength [89]. To address these limitations, our hydrogels incorporate polyphenols with catechol groups. This incorporation aims to mimic the adhesion properties observed in mussels. Mussels are aquatic invertebrates that produce adhesive proteins from their byssal gland [90]. These proteins have a high dopa content, which is produced through the modification of the tyrosine amino acid by the tyrosinase enzyme. By introducing catechol groups into our hydrogels, we aim to replicate the adhesive properties found in mussel proteins. The hydrogels made from hair keratin (dopamine and quercetin) demonstrated binding capability to Ti sheets. This interaction was facilitated by the hydrogel's catechol-containing catechol groups, which bound to the hydroxyl (OH) groups on the titanium oxide surface in **figure 4.15 (a1, a2)**. Furthermore, these hydrogels successfully adhered to PCL membranes and exhibited weightlifting capability by securely holding titanium sheet weights in **figure 4.15 (b1, b2), figure 4.16.** To fully assess the adhesive strength, additional testing using lap shear and other standard mechanical tests still needs to be conducted. These tests will provide a comprehensive evaluation of the adhesive strength of the hair keratin hydrogels and further validate their performance.

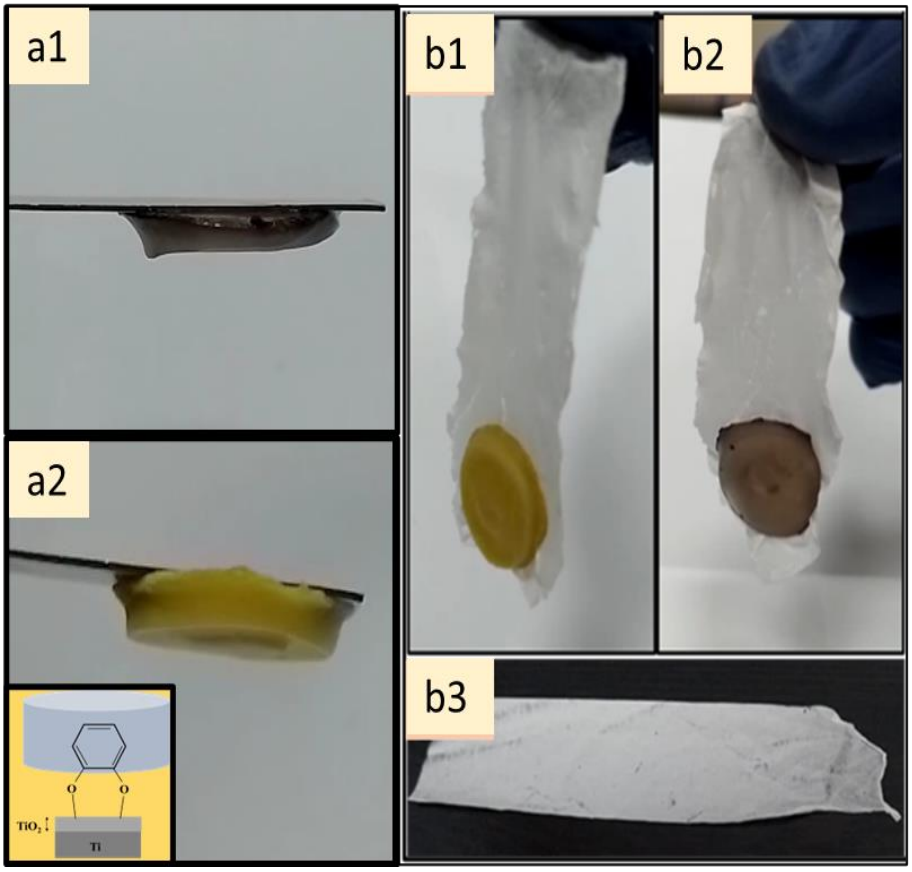

Figure 4.15: Adhesion of hydrogels to metallic titanium and skin tissue mimic (polycaprolactone membrane)

(a) Adhesion of the hydrogels to the titanium sheets. a1 - hair keratin dopamine hydrogel. a2 - hair keratin quercetin hydrogel, bonding between the titanium oxide layer over the Titanium metal to the catechol groups of the hydrogels.

(b) Adhesion to PCL membrane. b1 & b2 - adhesion between the PCL membrane to hair keratin quercetin hydrogel and to hair keratin dopamine hydrogel respectively. b3) Electro spun PCL membrane mimic like a natural skin.

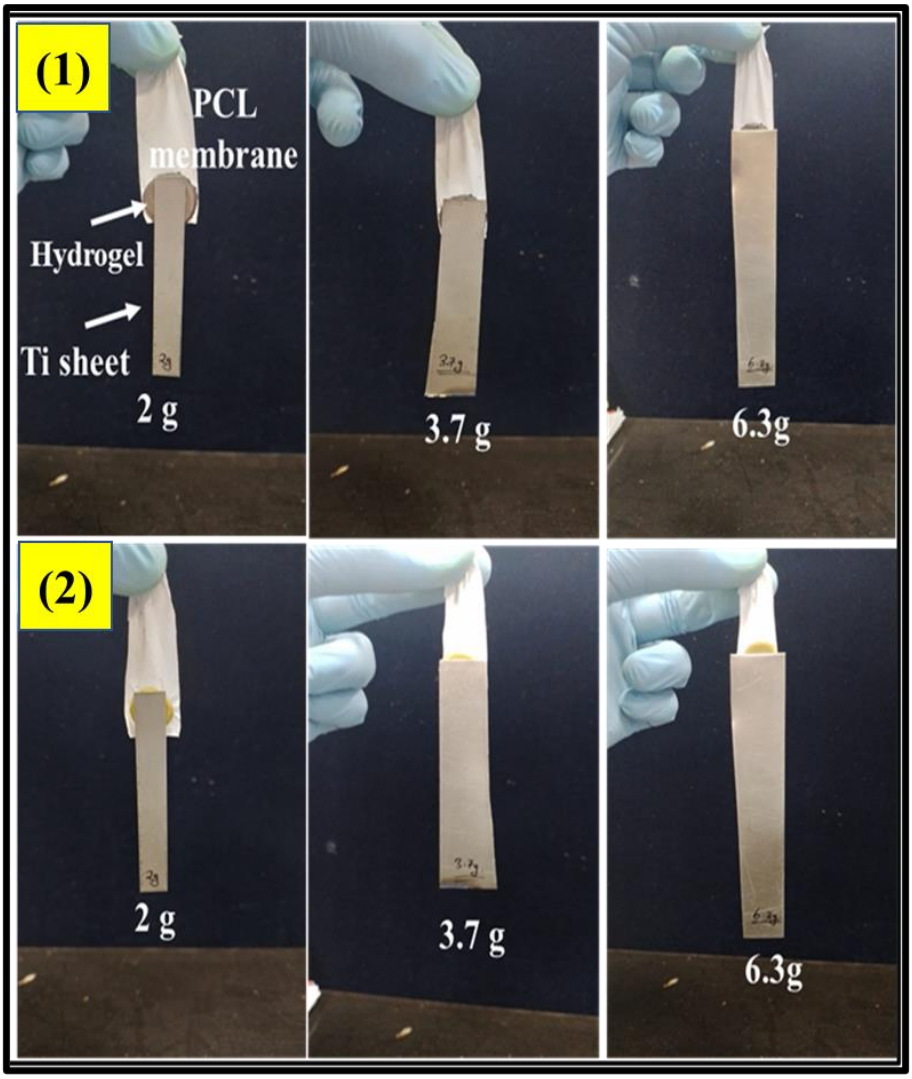

Figure 4.16: Semi-quantitative assessment of the adhesion strength of the hydrogels to titanium of different weights from PCL membrane (skin mimic).

4.7.6 Injectability of hydrogels

To assess the injectability of our hydrogels and their clinical relevance for injection or use as bio-ink in 3D bioprinting, various parameters including viscosity, storage modulus, and loss modulus were quantified using a rheometer were further checked by the

injectability testing. Common methods for injectability testing include force sensor or a material testing machine to measure injection force, allowing us to compare quantitatively the injectability of various hydrogels of differing material formulations [91]. In the absence of sophisticated machines, we employed a simpler approach to assess injectability. We manually applied mechanical pressure by gently pushing the syringe with our hand and gradually increasing the pressure until the hydrogels started to flow. The results obtained from this manual injectability testing were supported by the rheology data. As given in the **figure 4.17**, the injectability of the Hair Keratin-Quercetin hydrogels was lower compared to the Hair Keratin-Dopamine hydrogel. This observation is consistent with the rheology data, which showed a higher storage modulus (G') for the hair keratin dopamine hydrogel compared to the hair keratin quercetin hydrogels. The enhanced injectability of the hair keratin quercetin hydrogel can be attributed to the polymerization of dopamine, resulting in higher crosslinking and, consequently, higher viscosity and consistency of the hydrogel. Similarly, when attempting to draw an arbitrary shape using the hydrogel injection, the hair keratin dopamine hydrogel exhibited better performance with no breakage, while the hair keratin quercetin hydrogels experienced breakage under similar conditions. These results further highlight the superior injectability and structural integrity of the dopamine-based hydrogel compared to the quercetin gels.

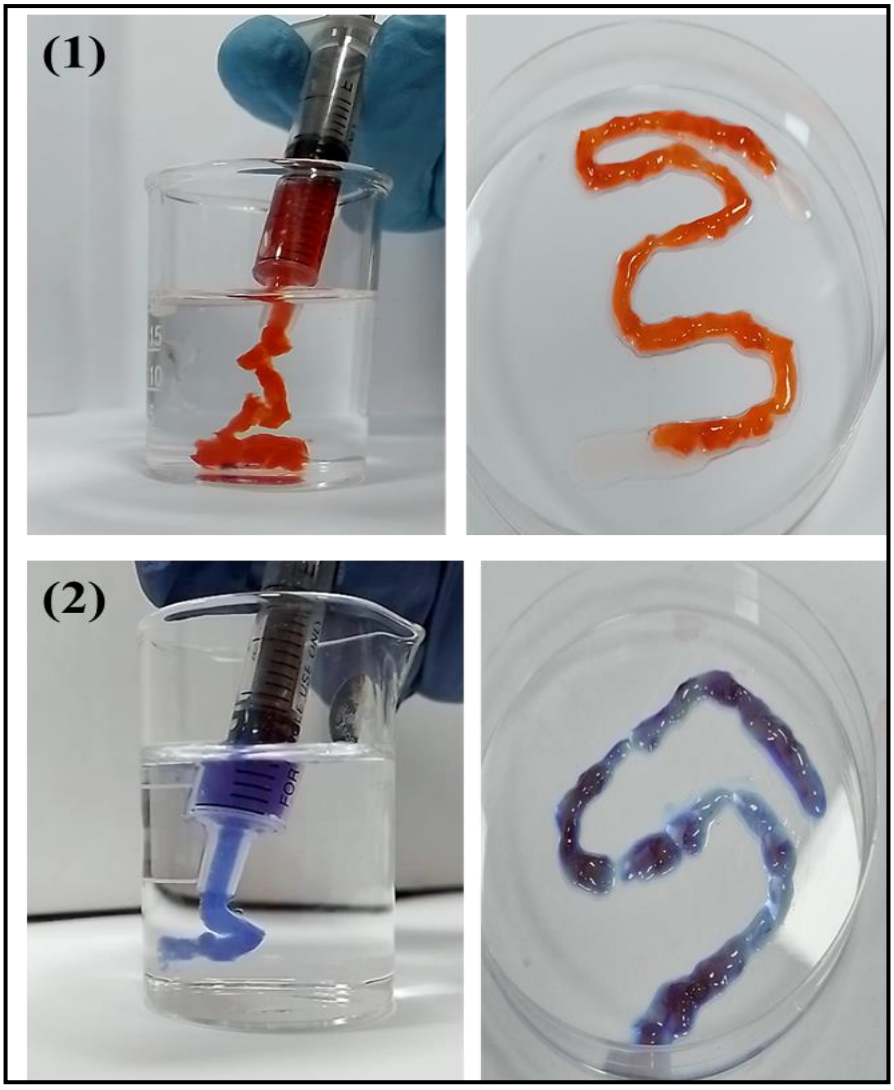

Figure 4.17: Injectability of hydrogels into aqueous media and dry surfaces. The test assesses the flow behaviour and thixotropic nature of the hydrogel under wet and dry conditions.

Chapter 5
Conclusion and future aspects

5.1 Conclusions

Medical devices are in increasing demand due to the increased life expectancy and advancement in medical techniques. Several devices such as stents, catheters, glucose sensors, needles, tracheal of food tubes and implants are available for assisting in human body functioning or monitoring purpose. These devices can replace or assist damaged body parts. One of the metallic implants, an osseointegrated percutaneous implant, creates a permanent barrier in skin and integrates to the bone. Such devices need proper integration of implant to bone along with the skin as well. Complication is associated with osseointegrated percutaneous implants such as epithelial downgrowth, immune response to the implanted foreign material, permigration (porous material) and mechanical avulsion (mechanical induced failure of implant). To address these problems various approaches have been studied. The conventional approach to seal the gap between the implant and skin is to suture, which affects the implant stability because this suture material is made of synthetic polymer. The use of traditional methods for wound closure like sutures, staples and flaps have certain disadvantages, particularly for delicate and vulnerable tissues. Tissue adhesives have been identified as a promising alternative for these purposes. They can also be used in combination with sutures in a highly wet environment when the tissue glue by itself cannot hold tissues together. To tackle the problem of wet adhesion, dopamine-based adhesives in recent years have attracted extensive interests as a promising material to improve wet adhesive performance. Tissue adhesives also have applications in hard tissue gluing, drug or cell delivery systems and cell culture. Their potential for the improvement of cell adhesion onto the surfaces is undeniable. Various types of

adhesives are commercially available in the market such as cyanoacrylate, which are not compatible to the host system and induce immune reactions and have low mechanical strength. In this thesis, hair keratin-based hydrogel is prepared from extracted keratin from human hair. Keratin was extracted using two different methods, sodium sulfide and urea-based method. Generally, hydrogel is formed with some crosslinking agents such as polyphenols (Dopamine and quercetin). Further extracted keratin was characterized by SDS-PAGE, FTIR and CD. This keratin was then utilized to fabricate a hydrogel using the catechol containing polyphenols. A significant visual variation in the hydrogel texture and morphology was observed upon increasing the mass ratio (m/m) of the protein:polyphenol which was due to the change in crosslinking density of the protein. Different combinations of hydrogels were prepared and characterized and analyzed for the rheological behavior, injectability and adhesion test. The developed hydrogel showed good shear thinning, injectability and self-healable behaviour. The keratin-based hydrogel as bioadhesive glue was fully biocompatible in nature. Overall, the developed injectable, biocompatible, dynamic hair keratin hydrogel with good adhesion strength could be effectively used as an emergent biomaterial for future biomedical application.

5.2 Future aspects

- Characterization and optimization of the adhesive strength of the quercetin and dopamine prepared hydrogels with hair keratin.
- To analyze the cytocompatibility of hydrogels with human skin derived fibroblasts and epidermal keratinocytes.
- To assess skin compatibility of the developed bioadhesive in vivo or ex vivo skin model.

References

[1] Jansen, J. A., Van Der Waerden, J. P. C. M., & De Groot, K. (1991). Development of a new percutaneous access device for implantation in soft tissues. Journal of biomedical materials research, 25(12), 1535-1545.

[2] Affeld, K., Grosshauser, J., Goubergrits, L., & Kertzscher, U. (2012). Percutaneous devices: a review of applications, problems and possible solutions. Expert Review of Medical Devices, 9(4), 389-399.

[3] Affeld, K., Grosshauser, J., Goubergrits, L., & Kertzscher, U. (2012). Percutaneous devices: a review of applications, problems and possible solutions. Expert Review of Medical Devices, 9(4), 389-399.

[4] Holgers, K. M., Bjursten, L. M., Thomsen, P., Ericson, L. E., & Tjellström, A. (1989). Experience with percutaneous titanium implants in the head and neck: a clinical and histological study. Journal of Investigative Surgery, 2(1), 7-16.

[5] Jayesh, R. S., & Dhinakarsamy, V. (2015). Osseointegration. Journal of pharmacy & bioallied sciences, 7(Suppl 1), S226.

[6] Hoellwarth, J. S., Tetsworth, K., Rozbruch, S. R., Handal, M. B., Coughlan, A., & Al Muderis, M. (2020). Osseointegration for amputees: current implants, techniques, and future directions. *JBJS reviews*, *8*(3).

[7] Overmann, A. L., & Forsberg, J. A. (2020). The state of the art of osseointegration for limb prosthesis. Biomedical engineering letters, 10, 5-16.

[8] Heaney, T. G., Doherty, P. J., & Williams, D. F. (1996). Marsupialization of percutaneous implants in presence of deep connective tissue. Journal of Biomedical Materials Research: An Official Journal of The Society for Biomaterials and The Japanese Society for Biomaterials, 32(4), 593-601.

[9] Fischer, N. G., & Aparicio, C. (2022). Junctional epithelium and hemidesmosomes: Tape and rivets for solving the “percutaneous device dilemma” in dental and other permanent implants. Bioactive Materials.

[10] Abdallah, M. N., Badran, Z., Ciobanu, O., Hamdan, N., & Tamimi, F. (2017). Strategies for optimizing the soft tissue seal around osseointegrated implants. Advanced healthcare materials, 6(20), 1700549.

[11] Cruz, M. B., Silva, N., Marques, J. F., Mata, A., Silva, F. S., & Caramês, J. (2022). Biomimetic implant surfaces and their role in biological integration—a concise review. Biomimetics, 7(2), 74.

[12] Pandey, C., Bhattarai, B. P., Riddhabhaya, A., Wongsirichat, N., & Rokaya, D. (2022). Healing Abutment Distortion in Implant Prostheses: An In Vitro Study. Journal of Functional Biomaterials, 13(3), 85.

[13] Al-Mubarak, L., & Al-Haddab, M. (2013). Cutaneous wound closure materials: an overview and update. Journal of cutaneous and aesthetic surgery, 6(4), 178.

[14] Li, M., Pan, G., Zhang, H., & Guo, B. (2022). Hydrogel adhesives for generalized wound treatment: design and applications. Journal of Polymer Science, 60(8), 1328-1359.

[15] Du, X., Wu, L., Yan, H., Qu, L., Wang, L., Wang, X., ... & Wang, L. (2019). Multifunctional hydrogel patch with toughness, tissue adhesiveness, and antibacterial activity for sutureless wound closure. ACS Biomaterials Science & Engineering, 5(5), 2610-2620

[16] Han, W., & Wang, S. (2022). Advances in Hemostatic Hydrogels That Can Adhere to Wet Surfaces. Gels, 9(1), 2.

[17] Mateescu, M., Baixe, S., Garnier, T., Jierry, L., Ball, V., Haikel, Y., ... & Lavalle, P. (2015). Antibacterial peptide-based gel for prevention of medical implanted-device infection. PLoS One, 10(12), e0145143.

[18] Cheng, H., Yue, K., Kazemzadeh-Narbat, M., Liu, Y., Khalilpour, A., Li, B., Zhang, Y.S., Annabi, N. and Khademhosseini, A., 2017. Mussel-inspired multifunctional hydrogel coating for prevention of infections and enhanced osteogenesis. ACS applied materials & interfaces, 9(13), pp.11428-11439.

[19] Bashir S, Hina M, Iqbal J, Rajpar AH, Mujtaba MA, Alghamdi NA, Wageh S, Ramesh K, Ramesh S. Fundamental concepts of hydrogels: Synthesis, properties, and their applications. Polymers. 2020 Nov 16;12(11):2702.

[20] Zezza, P., Lucío, M. I., Maquieira, Á., & Bañuls, M. J. (2022). DNA-based hydrogels for high-performance optical biosensing application. Talanta, 244, 123427.

[21] Cai, M. H., Chen, X. Y., Fu, L. Q., Du, W. L., Yang, X., Mou, X. Z., & Hu, P. Y. (2021). Design and development of hybrid hydrogels for biomedical applications: Recent trends in anticancer drug delivery and tissue engineering. Frontiers in Bioengineering and Biotechnology, 9, 630943.

[22] Hovgaard, L., & Brøndsted, H. (1995). Dextran hydrogels for colon-specific drug delivery. Journal of Controlled Release, 36(1-2), 159-166.

[23] Lee, D., Cho, S., Park, H. S., & Kwon, I. (2016). Ocular drug delivery through pHEMA-Hydrogel contact lenses Co-loaded with lipophilic vitamins. Scientific Reports, 6(1), 1-8.

[24] Liu, R., Xu, X., Zhuang, X., & Cheng, B. (2014). Solution blowing of chitosan/PVA hydrogel nanofiber mats. Carbohydrate polymers, 101, 1116-1121.

[25] Elviri, L., Bianchera, A., Bergonzi, C., & Bettini, R. (2017). Controlled local drug delivery strategies from chitosan hydrogels for wound healing. Expert opinion on drug delivery, 14(7), 897-908.

[26] Sudhakar, Y., Kuotsu, K., & Bandyopadhyay, A. K. (2006). Buccal bioadhesive drug delivery—a promising option for orally less efficient drugs. Journal of controlled release, 114(1), 15-40.

[27] Li, Z., Huang, S., Liu, Y., Yao, B., Hu, T., Shi, H., ... & Fu, X. (2018). Tuning alginate-gelatin bioink properties by varying solvent and their impact on stem cell behavior. Scientific reports, 8(1), 8020.

[28] Li, Z., Zhao, Y., Ouyang, X., Yang, Y., Chen, Y., Luo, Q., Zhang, Y., Zhu, D., Yu, X. and Li, L., 2022. Biomimetic hybrid hydrogel for hemostasis, adhesion prevention and promoting regeneration after partial liver resection. Bioactive Materials, 11, pp.41-51.

[29] Hasan, A., Khattab, A., Islam, M.A., Hweij, K.A., Zeitouny, J., Waters, R., Sayegh, M., Hossain, M.M. and Paul, A., 2015. Injectable hydrogels for cardiac tissue repair after myocardial infarction. Advanced Science, 2(11), p.1500122.

[30] Wang, X., Fang, X., Gao, X., Wang, H., Li, S., Li, C., Qing, Y. and Qin, Y., 2022. Strong adhesive and drug-loaded hydrogels for enhancing bone–implant interface fixation and anti-infection properties. Colloids and Surfaces B: Biointerfaces, 219, p.112817.

[31] Choe, G., Park, J., Park, H. and Lee, J.Y., 2018. Hydrogel biomaterials for stem cell microencapsulation. Polymers, 10(9), p.997.

[32] Yang, J. and Wang, S., 2023. Polysaccharide-based multifunctional hydrogel bio-adhesives for wound healing: a review. Gels, 9(2), p.138.

[33] Geckil, H., Xu, F., Zhang, X., Moon, S. and Demirci, U., 2010. Engineering hydrogels as extracellular matrix mimics. Nanomedicine, 5(3), pp.469-484.

[34] Li, X., Xu, Q., Johnson, M., Wang, X., Lyu, J., Li, Y., McMahon, S., Greiser, U., Sigen, A. and Wang, W., 2021. A chondroitin sulfate based injectable hydrogel for delivery of stem cells in cartilage regeneration. Biomaterials Science, 9(11), pp.4139-4148.

[35] Mauri, E., Sacchetti, A. and Rossi, F., 2016. The synthesis of RGD-functionalized hydrogels as a tool for therapeutic applications. JoVE (Journal of Visualized Experiments), (116), p.e54445.

[36] Yao, S., Xu, Y., Zhou, Y., Shao, C., Liu, Z., Jin, B., Zhao, R., Cao, H., Pan, H. and Tang, R., 2019. Calcium phosphate nanocluster-loaded injectable hydrogel for bone regeneration. ACS Applied Bio Materials, 2(10), pp.4408-4417.

[37] Koga, T., Kumazawa, S., Okimura, Y., Zaitsu, Y., Umeshita, K., & Asahina, I. (2020). Evaluation of Poly Lactic-co-Glycolic Acid-Coated β-Tricalcium Phosphate Bone Substitute as a Graft Material for Ridge Preservation after Tooth Extraction in Dog Mandible: A Comparative Study with Conventional β-Tricalcium Phosphate Granules. Materials, 13(16), 3452.

[38] Kim, S., Cui, Z. K., Kim, P. J., Jung, L. Y., & Lee, M. (2018). Design of hydrogels to stabilize and enhance bone morphogenetic protein activity by heparin mimetics. Acta biomaterialia, 72, 45-54.

[39] Jalageri, M. B., & Mohan Kumar, G. C. (2022). Hydroxyapatite Reinforced Polyvinyl Alcohol/Polyvinyl Pyrrolidone Based Hydrogel for Cartilage Replacement. Gels, 8(9), 555.

[40] Uma, K. (2023). Bioadhesives for clinical applications–a mini review. Materials Advances.

[41] Borie, E., Rosas, E., Kuramochi, G., Etcheberry, S., Olate, S., & Weber, B. (2019). Oral applications of cyanoacrylate adhesives: a literature review. BioMed research international, 2019.

[42] Walt, M. J., Atwood, N., Bernatchez, S. F., Ekholm, B. P., & Asmus, R. (2017). Skin protectants made of curable polymers: effect of application on local skin temperature. Advances in Wound Care, 6(4), 109-114.

[43] Panda, A., Kumar, S., Kumar, A., Bansal, R., & Bhartiya, S. (2009). Fibrin glue in ophthalmology. Indian journal of ophthalmology, 57(5), 371-379.

[44] Huang, H., Chen, H., Wang, X., Qiu, F., Liu, H., Lu, J., ... & Wu, H. (2019). Degradable and bioadhesive alginate-based composites: an effective hemostatic agent. ACS Biomaterials Science & Engineering, 5(10), 5498-5505.

[45] Zhang, Z., Wang, X., Wang, Y., & Hao, J. (2018). Rapid-forming and self-healing agarose-based hydrogels for tissue adhesives and potential wound dressings. Biomacromolecules, 19(3), 980-988.

[46] Hamedi, H., Moradi, S., Hudson, S. M., Tonelli, A. E., & King, M. W. (2022). Chitosan based bioadhesives for biomedical applications: A review. Carbohydrate Polymers, 119100.

[47] Li, C., Wang, T., Hu, L., Wei, Y., Liu, J., Mu, X., Nie, J. and Yang, D., 2014. Photocrosslinkable bioadhesive based on dextran and PEG derivatives. Materials Science and Engineering: C, 35, pp.300-306.

[48] Zhu, W., Peck, Y., Iqbal, J., & Wang, D. A. (2017). A novel DOPA-albumin based tissue adhesive for internal medical applications. Biomaterials, 147, 99-115.

[49] Brigham, M. D., Bick, A., Lo, E., Bendali, A., Burdick, J. A., & Khademhosseini, A. (2009). Mechanically robust and bioadhesive collagen and photocrosslinkable hyaluronic acid semi-interpenetrating networks. Tissue Engineering Part A, 15(7), 1645-1653.

[50] Gowda, A. H., Bu, Y., Kudina, O., Krishna, K. V., Bohara, R. A., Eglin, D., & Pandit, A. (2020). Design of tunable gelatin-dopamine based bioadhesives. International journal of biological macromolecules, 164, 1384-1391.

[51] Rathi, S., Saka, R., Domb, A. J., & Khan, W. (2019). Protein-based bioadhesives and bioglues. Polymers for Advanced Technologies, 30(2), 217-234.

[52] Bu, Y., & Pandit, A. (2022). Cohesion mechanisms for bioadhesives. Bioactive Materials, 13, 105-118.

[53] Rouse, J.G. and Van Dyke, M.E., 2010. A review of keratin-based biomaterials for biomedical applications. Materials, 3(2), pp.999-1014.

[54] Peng, Z., Mao, X., Zhang, J., Du, G., & Chen, J. (2020). Biotransformation of keratin waste to amino acids and active peptides based on cell-free catalysis. Biotechnology for biofuels, 13(1), 1-12.

[55] Feroz, S., Muhammad, N., Ratnayake, J., & Dias, G. (2020). Keratin-Based materials for biomedical applications. Bioactive materials, 5(3), 496-509.

[56]] McGovern, V. (2000). Recycling poultry feathers: more bang for the cluck. Environmental Health Perspectives, 108(8), A366-A369.

[57] Dan Mogosanu, G., Mihai Grumezescu, A., & Carmen Chifiriuc, M. (2014). Keratin-based biomaterials for biomedical applications. Current drug targets, 15(5), 518-530.

[58] Moll, R., Divo, M., & Langbein, L. (2008). The human keratins: biology and pathology. Histochemistry and cell biology, 129, 705-733.

[59] Aboushwareb, T., Eberli, D., Ward, C., Broda, C., Holcomb, J., Atala, A., & Van Dyke, M. (2009). A keratin biomaterial gel hemostat derived from human hair: evaluation in a rabbit model of lethal liver injury. Journal of Biomedical Materials Research Part B: Applied Biomaterials, 90(1), 45-54.

[60] Kang, H. J., Ko, N., Oh, S. J., An, S. Y., Hwang, Y. S., & Kim, S. Y. (2021). Injectable Human Hair Keratin–Fibrinogen Hydrogels for Engineering 3D Microenvironments to Accelerate Oral Tissue Regeneration. International Journal of Molecular Sciences, 22(24), 13269.

[61] Raja, S. T. K., Thiruselvi, T., Sailakshmi, G., Ganesh, S., & Gnanamani, A. (2013). Rejoining of cut wounds by engineered gelatin–keratin glue. Biochimica et Biophysica Acta (BBA)-General Subjects, 1830(8), 4030-4039.

[62] Unnikrishnan, G., & Ramasamy, V. (2020). Extraction of Keratin from Human Hair with Production of Biofertilizer from Waste Liquid of Hair Extraction and its Efficient Application on Growth Yield of Abelmoschus esculentus L. Asian Journal of Biological and Life Sciences, 9(2), 119.

[63] Wang, S., Taraballi, F., Tan, L. P., & Ng, K. W. (2012). Human keratin hydrogels support fibroblast attachment and proliferation in vitro. Cell and tissue research, 347, 795-802.

[64] Greenfield, N. J. (2006). Using circular dichroism spectra to estimate protein secondary structure. Nature protocols, 1(6), 2876-2890.

[65] Dietz, A. A., & Rubinstein, H. M. (1972). Standardization of the Ellman reaction. Clinical Biochemistry, 5(1-4), 136-138.

[66] Lv, Q., Wu, M., & Shen, Y. (2019). Enhanced swelling ratio and water retention capacity for novel super-absorbent hydrogel. Colloids and Surfaces A: Physicochemical and Engineering Aspects, 583, 123972.

[67] Ghosh, S., Ghosh, T., Bhowmik, S., Patidar, M. K., & Das, A. K. (2023). Nucleopeptide-coupled injectable bioconjugated guanosine-quadruplex hydrogel with inherent antibacterial activity. ACS Applied Bio Materials, 6(2), 640-651.

[68] Sadeghi-Avalshahr, A. R., Nokhasteh, S., Molavi, A. M., Mohammad-Pour, N., & Sadeghi, M. (2020). Tailored PCL scaffolds as skin substitutes using sacrificial PVP fibers and collagen/chitosan blends. International journal of molecular sciences, 21(7), 2311.

[69] Miyamoto, A., Kobayashi, K., Inomata, M., & Murakami, Y. (1982). Nitrogen-15 tracer investigation of the mechanism of the reaction of nitric oxide with ammonia on vanadium oxide catalysts. The Journal of Physical Chemistry, 86(15), 2945-2950.

[70] Tasaki, K. (2020). A novel thermal hydrolysis process for extraction of keratin from hog hair for commercial applications. Waste Management, 104, 33-41.

[71] Bertini, F., Canetti, M., Patrucco, A., & Zoccola, M. (2013). Wool keratin-polypropylene composites: Properties and thermal degradation. Polymer degradation and stability, 98(5), 980-987.

[72] Feroz, S., Muhammad, N., Ratnayake, J., & Dias, G. (2020). Keratin-Based materials for biomedical applications. Bioactive materials, 5(3), 496-509.

[73] Seghir, B. B., Hemmami, H., Zeghoud, S., Laouini, S. E., Rebiai, A., Amor, I. B., ... & Beki, A. (2020). Preparation methods keratin and nanoparticles keratin from wool: a review. Algerian Journal of Chemical Engineering AJCE, 1(1), 5-11.

[74] Nakamura, A., Arimoto, M., Takeuchi, K., & Fujii, T. (2002). A rapid extraction procedure of human hair proteins and identification of phosphorylated species. Biological and Pharmaceutical Bulletin, 25(5), 569-572.

[75] Wang, S., Taraballi, F., Tan, L. P., & Ng, K. W. (2012). Human keratin hydrogels support fibroblast attachment and proliferation in vitro. *Cell and tissue research*, *347*, 795-802.

[76] Hill, P., Brantley, H., & Van Dyke, M. (2010). Some properties of keratin biomaterials: kerateines. *Biomaterials*, *31*(4), 585-593.

[77] Jacob, J. T., Coulombe, P. A., Kwan, R., & Omary, M. B. (2018). Types I and II keratin intermediate filaments. Cold Spring Harbor perspectives in biology, 10(4), a018275.

[78] Shimomura, Y., & Ito, M. (2005, December). Human hair keratin-associated proteins. In Journal of Investigative Dermatology Symposium Proceedings (Vol. 10, No. 3, pp. 230-233). Elsevier.

[79] Greenfield, N. J. (2006). Using circular dichroism spectra to estimate protein secondary structure. Nature protocols, 1(6), 2876-2890.

[80] Miller, L. M., Bourassa, M. W., & Smith, R. J. (2013). FTIR spectroscopic imaging of protein aggregation in living cells. Biochimica et biophysica acta (BBA)-biomembranes, 1828(10), 2339-2346.

[81] Ellman, G. L. (1959). Quantitation of sulfhydrl DTNB, Ellman's reagent. Arch Biochem Biophys, 82, 70-7.

[82] Hu, W., Wang, Z., Xiao, Y., Zhang, S., & Wang, J. (2019). Advances in crosslinking strategies of biomedical hydrogels. Biomaterials science, 7(3), 843-855.

[83] Wang, Y., Jiao, A., Qiu, C., Liu, Q., Yang, Y., Bian, S., ... & Jin, Z. (2022). A combined enzymatic and ionic cross-linking strategy for pea protein/sodium alginate double-network hydrogel with excellent mechanical properties and freeze-thaw stability. Food Hydrocolloids, 131, 107737.

[84] Park, H., Guo, X., Temenoff, J. S., Tabata, Y., Caplan, A. I., Kasper, F. K., & Mikos, A. G. (2009). Effect of swelling ratio of injectable hydrogel composites on chondrogenic differentiation of encapsulated rabbit marrow mesenchymal stem cells in vitro. Biomacromolecules, 10(3), 541-546.

[85] Huang, W. S., & Chu, I. M. (2019). Injectable polypeptide hydrogel/inorganic nanoparticle composites for bone tissue engineering. PLoS One, 14(1), e0210285.

[86] Varchanis, S., Makrigiorgos, G., Moschopoulos, P., Dimakopoulos, Y., & Tsamopoulos, J. (2019). Modeling the rheology of thixotropic elasto-visco-plastic materials. Journal of Rheology, 63(4), 609-639.

[87]Alfieri, M. L., Weil, T., Ng, D. Y. W., & Ball, V. (2022). Polydopamine at biological interfaces. Advances in Colloid and Interface Science, 102689.

[88] Li, M., Pan, G., Zhang, H., & Guo, B. (2022). Hydrogel adhesives for generalized wound treatment: design and applications. Journal of Polymer Science, 60(8), 1328-1359.

[89] Pei, X., Wang, J., Cong, Y., & Fu, J. (2021). Recent progress in polymer hydrogel bioadhesives. Journal of Polymer Science, 59(13), 1312-1337.

[90] Liu, H., Qin, S., Liu, J., Zhou, C., Zhu, Y., Yuan, Y., ... & Wang, L. (2022). Bio-Inspired Self-Hydrophobized Sericin Adhesive with Tough Underwater Adhesion Enables Wound Healing and Fluid Leakage Sealing. Advanced Functional Materials, 32(32), 2201108.

[91] Chen, M. H., Wang, L. L., Chung, J. J., Kim, Y. H., Atluri, P., & Burdick, J. A. (2017). Methods to assess shear-thinning hydrogels for application as injectable biomaterials. ACS biomaterials science & engineering, 3(12), 3146-3160.